

**APPLICATION OF CONVOLUTION AND AVERAGE PRESSURE
APPROXIMATION FOR SOLVING NON-LINEAR FLOW PROBLEMS:
CONSTANT PRESSURE INNER BOUNDARY CONDITION FOR GAS FLOW**

A Thesis

by

MANSUR ZHAKUPOV

Submitted to the Office of Graduate Studies of
Texas A&M University
in partial fulfillment of the requirements for the degree of

MASTER OF SCIENCE

May 2005

Major Subject: Petroleum Engineering

**APPLICATION OF CONVOLUTION AND AVERAGE PRESSURE
APPROXIMATION FOR SOLVING NON-LINEAR FLOW PROBLEMS:
CONSTANT PRESSURE INNER BOUNDARY CONDITION FOR GAS FLOW**

A Thesis

by

MANSUR ZHAKUPOV

Submitted to the Office of Graduate Studies of
Texas A&M University
in partial fulfillment of the requirements for the degree of

MASTER OF SCIENCE

Approved as to style and content by:

Thomas A. Blasingame
(Chair of Committee)

Peter P. Valkó
(Member)

Steven L. Dorobek
(Member)

Stephen A. Holditch
(Head of Department)

May 2005

Major Subject: Petroleum Engineering

ABSTRACT

Application of Convolution and Average Pressure Approximation
for Solving Non-Linear Flow Problems:
Constant Pressure Inner Boundary Condition for Gas Flow. (May 2005)
Mansur Zhakupov,
Ingénieur de l'Ecole Polytechnique
Chair of Advisory Committee: Dr. Thomas A. Blasingame

The accurate description of fluid flow through porous media allows an engineer to properly analyze past behavior and predict future reservoir performance. In particular, appropriate mathematical models which describe fluid flow through porous media can be applied to well test and production data analysis. Such applications result in estimating important reservoir properties such as formation permeability, skin-factor, reservoir size, etc.

"Real gas" flow problems (*i.e.*, problems where the gas properties are specifically taken as implicit functions of pressure, temperature, and composition) are particularly challenging because the diffusivity equation for the "real gas" flow case is strongly non-linear. Whereas different methods exist which allow us to approximate the solution of the real gas diffusivity equation, all of these approximate methods have limitations. Whether in terms of limited applicability (say a specific pressure range), or due to the relative complexity (*e.g.*, iterative character of the solution), each of the existing approximate solutions does have disadvantages. The purpose of this work is to provide a solution mechanism for the case of time-dependent real gas flow which contains as few "limitations" as possible.

In this work, we provide an approach which combines the so-called average pressure approximation, a convolution for the right-hand-side non-linearity, and the Laplace transformation (original concept was put forth by Mireles and Blasingame). Mireles and Blasingame used a similar scheme to solve the real gas flow problem conditioned by the constant rate inner boundary condition. In this work we provide solution schemes to solve the constant pressure inner boundary condition problem. Our new semi-analytical solution was developed and implemented in the form of a direct (non-iterative) numerical procedure and successfully verified against numerical simulation.

Our work shows that while the validity of this approach does have its own assumptions (in particular, referencing the right-hand-side non-linearity to average reservoir pressure (similar to Mireles and Blasingame)), these assumptions are proved to be much less restrictive than those required by existing methods of solution for this problem. We believe that the accuracy of the proposed solution makes it

universally applicable for gas reservoir engineering. This suggestion is based on the fact that no pseudotime formulation is used. We note that there are pseudotime implementations for this problem, but we also note that pseudotime requires *a priori* knowledge of the pressure distribution in the reservoir or iteration on gas-in-place. Our new approach has no such restrictions.

In order to determine limits of validity of the proposed approach (*i.e.*, the limitations imposed by the underlining assumptions), we discuss the nature of the average pressure approximation (which is the basis for this work). And, in order to prove the universal applicability of this approach, we have also applied this methodology to resolve the time-dependent inner boundary condition for real gas flow in reservoirs.

ACKNOWLEDGEMENTS

I would like to sincerely thank the following:

Dr. Tom Blasingame for his knowledge, energy, openness, and clear understanding of the roles of all stakeholders in a successful venture, and thermodynamic peculiarities of the process of formation of one pure carbon crystalline modification.

Drs. Peter Valkó and Steve Dorobek for serving as members of my advisory committee.

Total S.A. for financial support of my graduate studies at Texas A&M University.

TABLE OF CONTENTS

	Page
CHAPTER I	INTRODUCTION..... 1
	1.1 Literature Review 1
	1.2 Previous Work..... 9
	1.3 Proposal for This Work 10
CHAPTER II	DEVELOPMENT OF AN ANALYTICAL PRESSURE SOLUTION FOR THE CASE OF A CONSTANT PRESSURE INNER BOUNDARY CONDITION 13
	2.1 General Approach..... 13
	2.2 Real-Gas Systems..... 14
	2.3 Key Relation..... 16
	2.4 Laplace and Inverse Laplace Transformations 17
CHAPTER III	VALIDATION OF THE PROPOSED CONSTANT PRESSURE SOLUTION AND THE AVERAGE PRESSURE APPROXIMATION: A DIRECT PROCEDURE FOR PERFORMANCE PREDICTION 19
	3.1 Verification Based on Numerical Simulator Outputs — Verification of Pressure Profiles..... 19
	3.2 Forward Modeling (Performance Prediction)..... 22
	3.3 Alternative Deliverability Equations 33
CHAPTER IV	EXTENSIONS 37
	4.1 Initial Attempts to Model a Variable Pressure Schedule 37
	4.2 Time-Dependent Inner Boundary Condition (Variable Pressure Schedule)..... 38
CHAPTER V	SUMMARY, CONCLUSIONS, AND RECOMMENDATIONS FOR FUTURE WORK 42
	5.1 Summary 42
	5.2 Conclusions 43
	5.3 Recommendations for Future Work 44
NOMENCLATURE 45
REFERENCES 47

	Page
APPENDIX A ANALYTICAL PRESSURE SOLUTION FOR THE CASE OF A CONSTANT PRESSURE INNER BOUNDARY CONDITION	50
APPENDIX B NON-LINEARITY AND AVERAGE PRESSURE APPROXIMATION	54
APPENDIX C ADAPTED ROUMBOUTSOS AND STEWART NUMERICAL LAPLACE TRANSFORM ALGORITHM	58
APPENDIX D ALGORITHMS FOR VERIFICATION AND PERFORMANCE PREDICTION: ACCURACY AND COMPUTATIONAL TIME CONSIDERATIONS	61
VITA.....	64

LIST OF TABLES

TABLE		Page
3.1	System Parameters for Pressure Profiles Validation Cases.....	20
3.2	Gas Properties	23
3.3	Mireles and Blasingame Set of Reservoir Properties (Type 1)	23
3.4	Reservoir Properties (Type 2)	23
3.5	Flowing Bottomhole Pressure Schedules (Used in Performance Prediction).....	24
4.1	Flowing Bottomhole Pressure Schedules (Used in Initial Attempts to Model a Variable Pressure Schedule)	38
4.2	Flowing Bottomhole Pressure Schedules (Used in Application of a Rigorous Solution Formulation for a Variable Pressure Schedule).....	41

LIST OF FIGURES

FIGURE	Page
1.1a Cartesian plot of the $p/\mu z$ product versus pressure for a set of gas gravity values ($T = 200^\circ\text{F}$)	3
1.1b Log-log plot of the $p/\mu z$ product versus pressure for a set of gas gravity values ($T = 200^\circ\text{F}$)...	3
1.2a Cartesian plot of the μc product versus pressure for a set of gas gravity values ($T = 200^\circ\text{F}$)....	4
1.2b Log-log plot of the μc product versus pressure for a set of gas gravity values ($T = 200^\circ\text{F}$).....	4
1.3a Cartesian plot of the μz product versus pressure for a set of gas gravity values ($T = 200^\circ\text{F}$)....	6
1.3b Log-log plot of the μz product versus pressure for a set of gas gravity values ($T = 200^\circ\text{F}$).....	6
1.4 Mireles and Blasingame ¹ application of convolution (<i>i.e.</i> , superposition of "unit" rate solutions) for constructing the constant rate solution. This is not universal (or even practical) approach — it is an <i>a posteriori</i> adjustment using the APA (incorrectly) for the constant pressure case.	11
3.1 Dimensionless pseudopressure profile at $t = 17.14$ D for the reservoir system presented in Table 3.1	21
3.2 Dimensionless pseudopressure profile at $t = 22.23$ D for the reservoir system presented in Table 3.1	21
3.3 Fetkovich-Carter "composite" rate type curve — zoom view (Type 1 and 2 cases, $r_{eD} = 10^2$)	26
3.4 Fetkovich-Carter "composite" rate type curve — zoom view (Type 1 and 2 cases, $r_{eD} = 10^3$)	27
3.5 Fetkovich-Carter "composite" rate type curve — zoom view (Type 1 and 2 cases, $r_{eD} = 10^4$)	28
3.6 Fetkovich-Carter "composite" rate type curve — zoom view (Type 1 and 2 cases, superposition of $r_{eD} = 10^2, 10^3, 10^4$)	29
3.7 Fetkovich-Carter "composite" rate type curve — global view (Type 1 and 2 cases, superposition of $r_{eD} = 10^2, 10^3, 10^4$)	30
3.8 Fetkovich-Carter "composite" rate type curve — zoom view of timestep-related convergence (Type 1 and 2 cases, $r_{eD} = 10^3$)	32
3.9 Comparison of rates predicted by coupling our solution with Darcy's law and PSS deliverability equation.....	34
3.10 Semilog comparison of pressure profiles predicted by coupling our solution with Darcy's law and PSS deliverability equation.....	35

FIGURE	Page
3.11 Log-log comparison of pressure profiles predicted by coupling our solution with Darcy's law and the PSS deliverability equation.....	35
4.1 Comparison of "simplistic" strategies used to generate production profiles for the variable bottomhole flowing pressure case.....	38
4.2 Pressure profile comparison computed based on flowrate profiles obtained from numerical simulation for the variable flowing bottomhole pressure case.....	41
B-1 Typical profile of β -function during production (for both constant pressure and constant rate inner boundary conditions).....	57

CHAPTER I

INTRODUCTION

1.1 Literature Review

From a historical perspective, petroleum engineers have developed numerous systematic methods to qualitatively and quantitatively assess production from gas reservoirs. Several approaches for modeling gas flow through porous media have been proposed independently, or adapted from such fields as theory of heat conduction, which is governed by similar partial differential equations and, in the case of heat flow in particular, and electrical flow and mass transfer in general, these are more mature fields of science. Indeed, *similarities* and *analogies* are very powerful tools, and many solutions used in petroleum engineering were developed or extracted from the classical works on heat conduction of Carslaw and Jaeger,²⁻³ and Jaeger⁴ (as one very relevant example).

For the case of fluid flow in porous media, the governing partial differential equation is of parabolic type, and is known as the diffusivity equation for pressure. The diffusivity equation can be readily derived by combining a continuity equation (mass balance), a flow equation (momentum balance), and an equation of state (dependence of thermodynamic properties on pressure and temperature).

The existence and uniqueness of solutions for the diffusivity equation have been demonstrated for a wide set of boundary and initial conditions — particularly for conditions which petroleum engineers typically face (constant rate or pressure at the well (inner boundary); infinite-acting, no-flow, or constant pressure outer boundaries). In general terms we can specify flow (Neumann-type) or pressure (Dirichlet-type) boundary conditions and smooth initial pressure distributions (in particular, the most popular initial condition is that of a uniform (or constant) pressure distribution).⁵

The main difficulty in resolving the diffusivity equation for the gas flow case is the pressure dependence of its parameters — *i.e.*, the non-linear character of the equation. In its general form, the diffusivity equation for flow in porous media is given by:

$$\operatorname{div} \left[\frac{p}{\mu z} \nabla p \right] = \frac{\phi c}{k} \frac{p}{z} \frac{\partial p}{\partial t} \dots\dots\dots (1.1)$$

For clarity, and without loss of generality, we formulate the problem in terms of effective "gas" porosity. Refer to Section 2.2 for an extended definition.

This thesis follows the style and format of the *SPE Journal*.

Non-trivial, closed-form solutions do not exist for Eq. 1.1, but a few methods can be used to generate reasonable approximations to the non-linear solutions⁶ (which are typically computed numerically). We recognize that the pressure dependence of the thermodynamic properties is well understood, but this knowledge does not necessarily translate into a viable non-linear solution (*i.e.*, one can not simply substitute some convenient form of the thermodynamic properties and hope for an approximate solution). However, several elegant (and quite efficient) approximations for the diffusivity equation have been proposed and validated for certain pressure ranges.

Let us start with the simplest problem of fluid mechanics in porous media — that of single-phase "slightly compressible" *liquid* flow. The diffusivity equation constructed under such assumptions is linear since its parameters are assumed constant (which joined with the assumption of a small compressibility is the very definition of being "slightly compressible"):

$$\nabla^2 p = \frac{\phi\mu c}{k} \frac{\partial p}{\partial t} \dots\dots\dots (1.2)$$

In 1949 van Everdingen and Hurst⁷ applied the Laplace transformation to solve Eq. 1.2 in radial coordinates for the constant rate and constant pressure inner boundary conditions. For the infinite-acting outer boundary condition we have:

$$\bar{p}_D(u, r_D) = \frac{1}{u} \frac{K_0(\sqrt{u}r_D)}{\sqrt{u}K_1(\sqrt{u})} \quad (\text{constant rate})\dots\dots\dots (1.3)$$

$$\bar{q}_D(u) = \frac{1}{u} \frac{K_1(\sqrt{u})}{\sqrt{u}K_0(\sqrt{u})} \quad (\text{constant wellbore pressure}) \dots\dots\dots (1.4)$$

And for a bounded circular reservoir (no-flow outer boundary):

$$\bar{p}_D(u, r_D) = \frac{1}{u} \frac{I_0(\sqrt{u}r_D)K_1(\sqrt{u}r_{eD}) + I_1(\sqrt{u}r_{eD})K_0(\sqrt{u}r_D)}{\sqrt{u}I_1(\sqrt{u}r_{eD})K_1(\sqrt{u}) - \sqrt{u}I_1(\sqrt{u})K_1(\sqrt{u}r_{eD})} \quad (\text{constant rate})\dots\dots\dots (1.5)$$

$$\bar{q}_D(u) = \frac{1}{u} \frac{I_1(\sqrt{u}r_{eD})K_1(\sqrt{u}) - I_1(\sqrt{u})K_1(\sqrt{u}r_{eD})}{\sqrt{u}I_0(\sqrt{u})K_1(\sqrt{u}r_{eD}) + \sqrt{u}I_1(\sqrt{u}r_{eD})K_0(\sqrt{u})} \quad (\text{constant wellbore pressure})\dots\dots\dots (1.6)$$

The use of solutions for the "linear" (or liquid) diffusivity equation to gas flow problems was advocated by Matthews and Russell⁸ in 1967. The applicability of the "liquid" solutions to gas flow systems relies upon assumptions which require the behavior of the μc and the $p/\mu z$ products to remain constant with pressure. It has been suggested that for pressures greater than 2000 psia the $p/\mu z$ product is relatively constant (**Figs. 1.1a and 1.1b**) — and for similar ranges of pressures the μc product varies slowly (**Figs. 1.2a and 1.2b**).

We note that the "long-time" linear (or liquid) solution for bounded reservoirs yields an exponential rate decline:

$$q = q_i \exp(-D_i t) \dots\dots\dots (1.7)$$

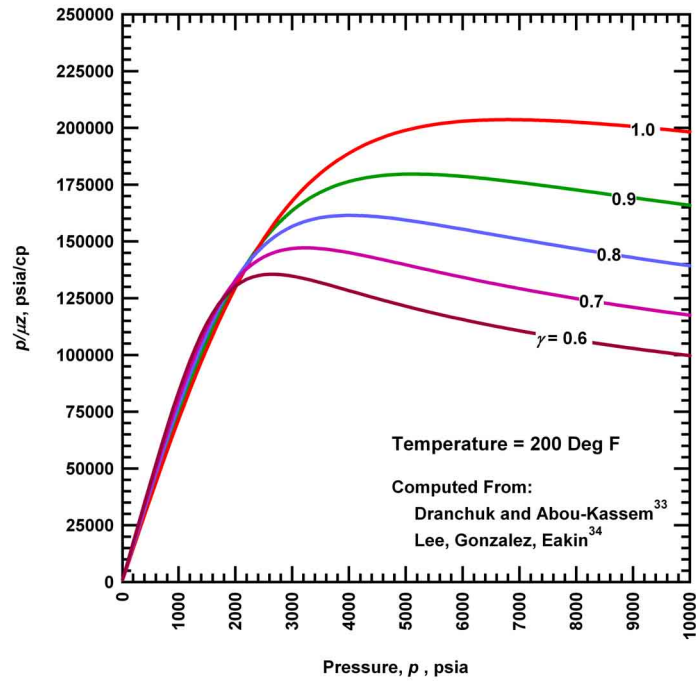


Figure 1.1a — Cartesian plot of the $p/\mu z$ product versus pressure for a set of gas gravity values ($T = 200^\circ\text{F}$).

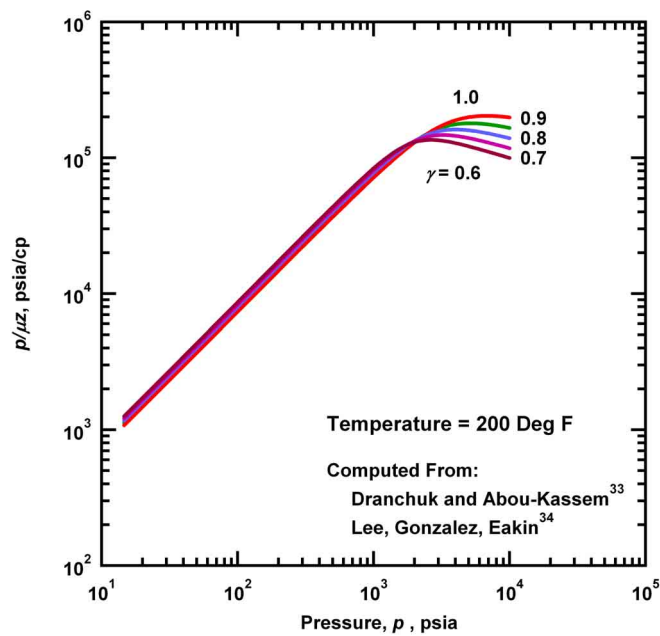


Figure 1.1b — Log-log plot of the $p/\mu z$ product versus pressure for a set of gas gravity values ($T = 200^\circ\text{F}$).

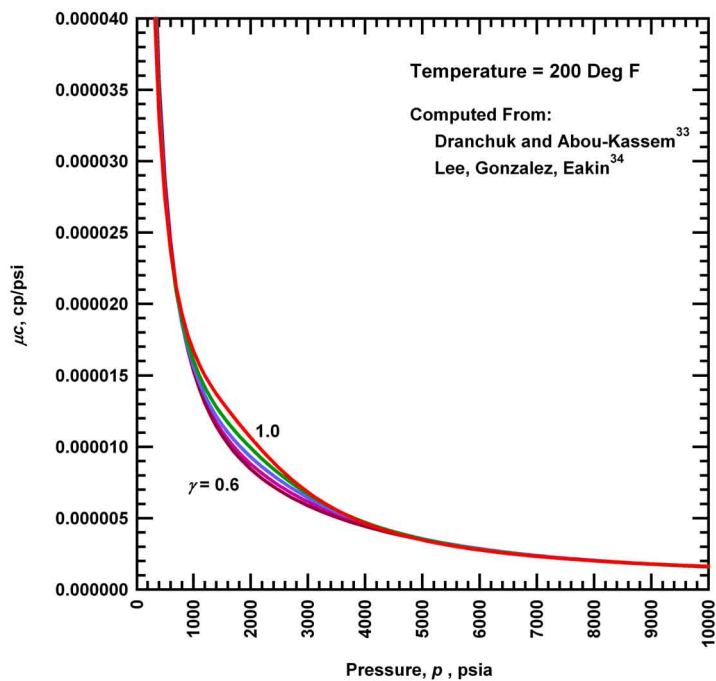


Figure 1.2a — Cartesian plot of the μc product versus pressure for a set of gas gravity values ($T = 200^\circ\text{F}$).

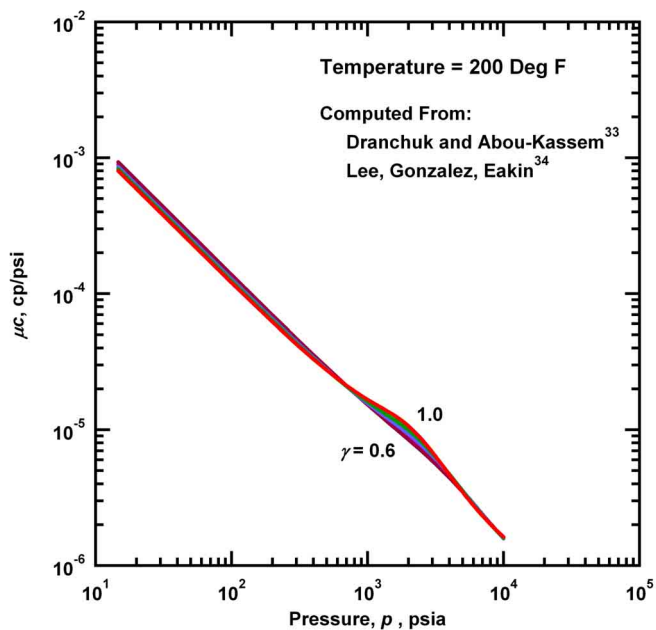


Figure 1.2b — Log-log plot of the μc product versus pressure for a set of gas gravity values ($T = 200^\circ\text{F}$).

Strictly speaking, the "pressure" formulation, or p -method as it is known, in general form is given by:

$$\nabla^2 p - \frac{\partial}{\partial p} \left[\ln \left[\frac{\mu c}{p} \right] \right] (\nabla p)^2 = \frac{\phi \mu c}{k} \frac{\partial p}{\partial t} \quad (1.8)$$

which reduces to:

$$\nabla^2 p = \frac{\phi \mu c}{k} \frac{\partial p}{\partial t} \quad (1.9)$$

if $p/\mu c$ product is assumed constant. Note that the μc product was *not* assumed constant in the transition from Eq. 1.8 to Eq. 1.9. Nevertheless, as shown in **Figs. 1.2a and 1.2b**, the μc product varies *slowly* over small pressure drawdowns in the range of high pressures; in other cases the use of liquid solution is not valid, and the right-hand side of Eq. 1.9 would also have to be linearized.

Current practice suggests that the best technique for resolving the non-linear diffusivity equation (Eq. 1.1) is to recast this equation into a linear formulation (via the transformations known as pseudopressure and pseudotime). Consequently, constructing linear solutions is a major topic for gas reservoir engineering — however, as this not the primary objective of this work, we have chosen not to concentrate our attention (or literature review) on linear solutions, but rather on ideas intrinsic to gas flow systems. As one method of solving linear partial diffusivity equations, we simply mention the Boltzmann transformation as an alternative way of constructing analytical (and/or semi-analytical) solutions for a linear diffusivity equation.

Another case of particular interest is that case where the product of the viscosity and total compressibility (μc) is (can be assumed) constant. Here the diffusivity equation for describing gas flow can be expressed in terms of "pressure-squared" as follows, in general form:

$$\nabla^2 (p^2) - \frac{\partial}{\partial p^2} [\ln(\mu c)] \nabla (p^2)^2 = \frac{\phi \mu c}{k} \frac{\partial}{\partial t} (p^2) \quad (1.10)$$

and in linearized form:

$$\nabla^2 (p^2) = \frac{\phi \mu c}{k} \frac{\partial p^2}{\partial t} \quad (1.11)$$

Being in a sense complementary to the p -method ("liquid" solutions), the p^2 -method is only applicable for low pressures — the range of pressures between 0 and 2000 psia is most often quoted — because the μc product appears constant for low pressures (**Figs. 1.3a and 1.3b**). Again, the μc product was not assumed constant in transition from Eq. 1.10 to Eq. 1.11. However, if the μc product is essentially constant — taking into account **Figs. 1.2a and 1.2b**, for pressures less than 2000 psia, the μc product can be assumed constant only for cases of small drawdowns — we can use "liquid" solutions.

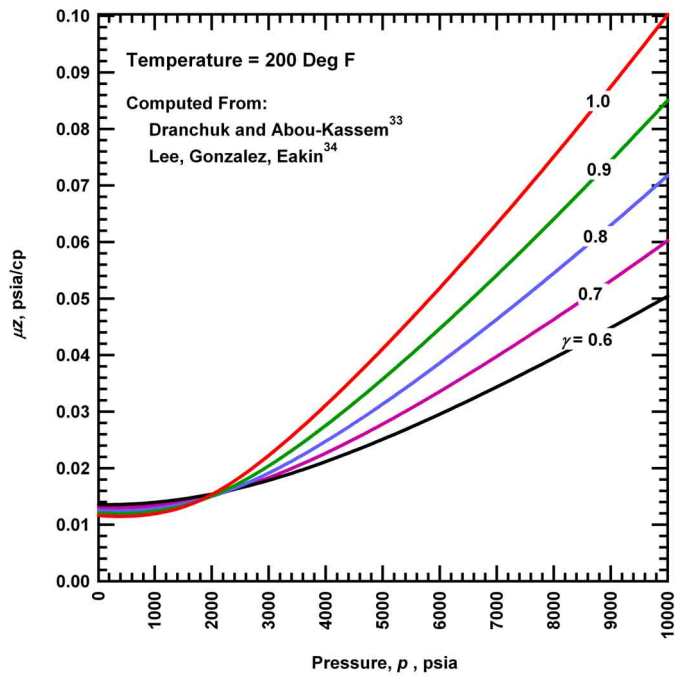


Figure 1.3a — Cartesian plot of the μz product versus pressure for a set of gas gravity values ($T = 200^\circ\text{F}$).

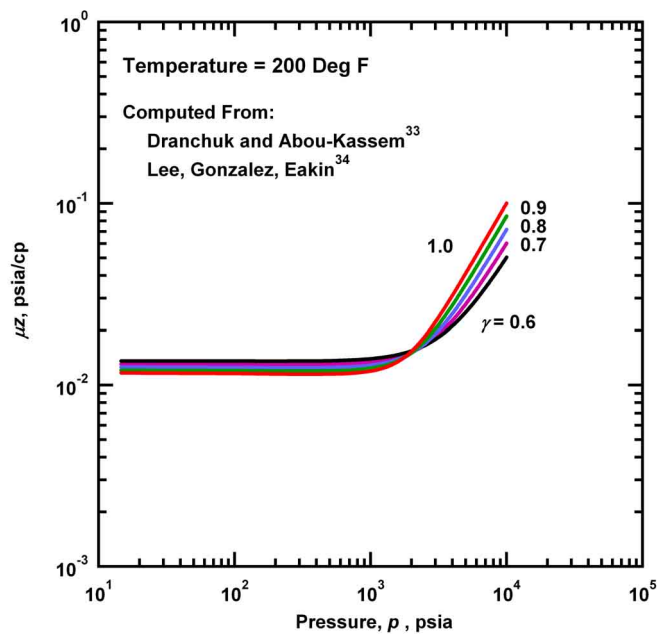


Figure 1.3b — Log-log plot of the μz product versus pressure for a set of gas gravity values ($T = 200^\circ\text{F}$).

As we noted earlier, a very important concept for application is to completely linearize the diffusivity equation and to use the corresponding linear (liquid) flow solutions. Two transformations were proposed — pseudopressure and pseudotime (although pseudotime is still not fully understood⁶). Pseudotime, which is used to linearize the right-hand side of the diffusivity equation can be combined with pseudopressure to provide a "complete" linearization. We could (in theory) combine pseudotime with the p - and p^2 -methods of the diffusivity equation within the ranges of validity of the latter. However, this would not be a practical result — moreover, Aziz, *et al.*⁹ showed by comparison that pseudopressure was the most reliable choice for pressure drawdown analysis of gas reservoirs.

The pseudopressure is nothing else than Kirchhof transformation well known in heat theory. Its purpose is to account for the variation of the μz product as a function of pressure (constant permeability is assumed). Thus, in 1966 Al-Hussainy, Ramey and Crawford¹⁰ introduced the "real gas pseudopressure" function:

$$m(p) = 2 \int_{p_0}^p \frac{p}{\mu z} dp \dots\dots\dots (1.12)$$

which has units of psi^2/cp and by construction is universally valid. As Raghavan⁶ pointed out the multiplier of 2 is due to the fact that if the μz product is constant, then $m(p) = ap^2/2$, where $a = 1/(\mu z)$.

Although this is rather a question of style, we follow Mireles and Blasingame¹ and define pseudopressure for the purpose of the present work as follows:

$$m(p) = \frac{\mu_i z_i}{p_i} \int_{p_{base}}^p \frac{p}{\mu z} dp \dots\dots\dots (1.13)$$

In any case, by incorporating pseudopressure into the diffusivity equation, the spatial constituent (laplacian) of the diffusivity equation is linearized:

$$\nabla^2 m = \frac{\phi \mu c}{k} \frac{\partial m}{\partial t} \dots\dots\dots (1.14)$$

In 1979 Agarwal¹¹ introduced a new transformation known as pseudotime for the analysis of pressure buildup data in gas reservoirs. He found that the use of pseudotime for pressure buildup tests and application of the drawdown solutions available for liquid systems yielded correct results. The definition of pseudotime, which provides an approximate linearization of the diffusivity equation by accounting for the μc term and its variation with pressure, is as follows (here normalized):

$$t_a(t) = \mu_i c_i \int_{t_0}^t \frac{dt}{\mu c} \dots\dots\dots (1.15)$$

Pseudopressure-pseudotime formulation completely linearizes the diffusivity equation:

$$\nabla^2 m = \frac{\phi \mu_i c_i}{k} \frac{\partial m}{\partial t_a} \dots\dots\dots (1.16)$$

As opposed to pseudopressure, pseudotime is an approximate function. It assumes that time and pressure vary linearly with time over sufficiently small time increments. Nevertheless, the use of pseudopressure usually provides accurate results.

Different authors compared methods described above in sense of applicability to gas flow problems.^{9,12} The conclusion is that the pseudopressure form of the diffusivity equation should be used. Moreover, in cases where the μc product varies significantly both pseudopressure and pseudotime are to be applied.

An alternative way of resolving non-linear partial differential equations consists in application of a so called perturbation technique. In 1980 Kale and Mattar¹³ applied the perturbation technique to the real gas diffusivity equation. Their solution (for constant rate inner boundary condition) is given by:

$$p_{pD}^{\circ} = p_D + \delta \dots\dots\dots (1.17)$$

where p_D is the solution for "slightly compressible" fluid:

$$p_D = \frac{1}{2} E_1 \left[\frac{1}{2.637 \times 10^4} \frac{\phi \mu_i c_i r^2}{4kt} \right] \dots\dots\dots (1.18)$$

and δ is the correction term developed by assuming that certain second-order terms and higher-order differentials in the partial differential equation were negligible:

$$\delta = \frac{1}{2} \int_{\infty}^x \frac{\alpha \exp(-x)}{1+x} dx \dots\dots\dots (1.19)$$

The parameters are defined as follows:

$$x = \frac{r_D^2}{4t_D} \dots\dots\dots (1.20)$$

$$\alpha = \frac{\mu c - \mu_i c_i}{\mu_i c_i} \dots\dots\dots (1.21)$$

Note that this solution can be difficult to apply. One will also recognize Boltzmann transformation in Eq. 1.20. In 1986 Kabir and Hasan¹⁴ proposed another expression for the correction term:

$$\delta = \frac{1}{2} \int_{\infty}^x \frac{\alpha \exp(-x)}{1+x+\alpha x} dx \dots\dots\dots (1.22)$$

As distinct from Kale and Mattar they did not neglect any second order terms.

Also in 1986 Aadnoy and Finjord¹⁵ underlined the importance of including the higher-order differentials while proposing to neglect second-order terms in the correction term:

$$\delta = -\frac{1}{2} \int_{\infty}^x \frac{\exp(-y)}{y} dy \int_0^y \alpha(z) dz \dots\dots\dots (1.23)$$

Other authors developed similar solutions using perturbation technique.¹⁶⁻¹⁷

Now, the diffusivity equation is formulated in terms of pressure. So if the inner boundary condition specifies rate, after resolving the equation we know both rate and pressure distribution at any time. If the inner boundary condition specifies pressure, then resolving the diffusivity equation alone does not yield rate. The obvious way to obtain the latter is to couple the diffusivity equation with a deliverability equation. Darcy's law will be the correct choice if the flow equation used in derivation of the diffusivity equation was also Darcy-based.

An alternative approach for pressure inner boundary condition is not to resolve the diffusivity equation coupled with a deliverability equation, but to propose gas flow relations. We can mention the "backpressure" equation, and Arps,¹⁸ Fetkovich,¹⁹ Ansah, *et al.*,²⁰ and Buba²¹ relations.

We will retain limitations of the existing methods:

- Diffusivity-Equation-Based: Restrictive assumptions, and tedious iterative character of pseudotime.
- Gas-Flow-Relation-Based: Being by construction non-universal, and predicting only rate and not pressure distribution.

1.2 Previous Work

Mireles and Blasingame¹ developed an original closed form Laplace domain solution for the flow of a real gas from a well producing at a *constant rate* in a bounded circular reservoir. More importantly, they proposed a new approach that uses pseudopressure to linearize the spatial portion of the diffusivity equation and uses convolution to account for the pressure-dependent non-linear term in the time portion of it. Consequently, their semi-analytical solution eliminated the use of pseudotime.

However, although being rigorous their solution relies on evaluation of the non-linear term based on the average reservoir pressure predicted from material balance. They did not really assess the nature and applicability of the average pressure approximation (APA). Nevertheless, the APA worked perfectly for their case of a constant rate inner boundary condition as confirmed by numerical simulation. This fact may be considered as an empirical demonstration of validity of the APA for all (realistic) values of pressure.

Again, the need for such a solution arises in the analysis of gas well test data and gas well production data, where both analyses currently use approximate methods such as the pressure or pressure-squared methods,²²⁻²³ or rigorous, but tedious pseudovariabes.¹⁰⁻¹¹

Concisely, Mireles and Blasingame showed that for the boundary condition specified above and for the uniform initial condition the equation of diffusivity (here in an appropriate dimensionless form):

$$\frac{1}{r_D} \frac{\partial}{\partial r_D} \left[r_D \frac{\partial m_D}{\partial r_D} \right] = \frac{\mu c}{\mu_i c_i} \frac{\partial m_D}{\partial t_D} \dots\dots\dots (1.24)$$

allows the following Laplace domain solution:

$$\bar{m}_{D,gas} = \bar{g}(u)\bar{m}_D(ug(u)) \dots\dots\dots (1.25)$$

where $\bar{m}_{D,gas}$ is the solution of the "liquid" problem (which can be written in analytical form for the stated boundary conditions), non-linearity of the problem is represented by (reduced to):

$$\mathcal{L}[g(t_D)] \equiv \bar{g}(u) = \frac{1}{u} \frac{1}{\mathcal{L}\left[\frac{1}{\beta_{\bar{p}}}(t_D)\right]} \dots\dots\dots (1.26)$$

and the APA is used to calculate:

$$\beta_{\bar{p}} = \frac{\bar{\mu}c}{\mu_i c_i} \dots\dots\dots (1.27)$$

Note that in this case of constant rate inner boundary condition $\bar{g}(u)$ depends only on the value of β -function calculated at average pressure. Since the rate is known, the average pressure and therefore $\beta_{\bar{p}}$ can be easily forecasted even before resolving the equation.

Their final step was to propose functional and numerical models to calculate $\bar{g}(u)$. A numerical model consisted in applying the Roumboutsos and Stewart²⁴ algorithm to transform the data (forecasted as described in the previous paragraph) into Laplace domain. Finally, the Stehfest²⁵ algorithm was chosen for the inverse transformation of the Laplace domain solution given by Eq. 1.25.

1.3 Proposal for This Work

We began our work by implementing Mireles and Blasingame¹ approach and essentially confirming their results. In particular, p_{wf} versus time during transient periods was correctly predicted.

A logical continuation of their work is to develop a closed form Laplace domain solution for the flow of a real gas from a well producing at a *constant pressure* in a bounded reservoir — constant pressure inner boundary condition being also often used for production control — using pseudopressure, convolution, and the APA. Since the approach should predict both pressures and rates, coupling with deliverability equations has to be considered.

Mireles and Blasingame gave a few hints to investigators seeking a solution for a constant pressure boundary condition. In particular, they questioned applicability of convolution (superposition) which is to say a standard way of constructing a solution for a linear constant pressure condition problem based on an available linear constant rate condition solution. Indeed, although the approach based on convolution and the APA linearizes the diffusivity equation in a sense, convolution did not work (**Fig. 1.4**). They suggested recasting the diffusivity equation specifically for the case of constant pressure condition and conjectured a need to start from fundamentals.

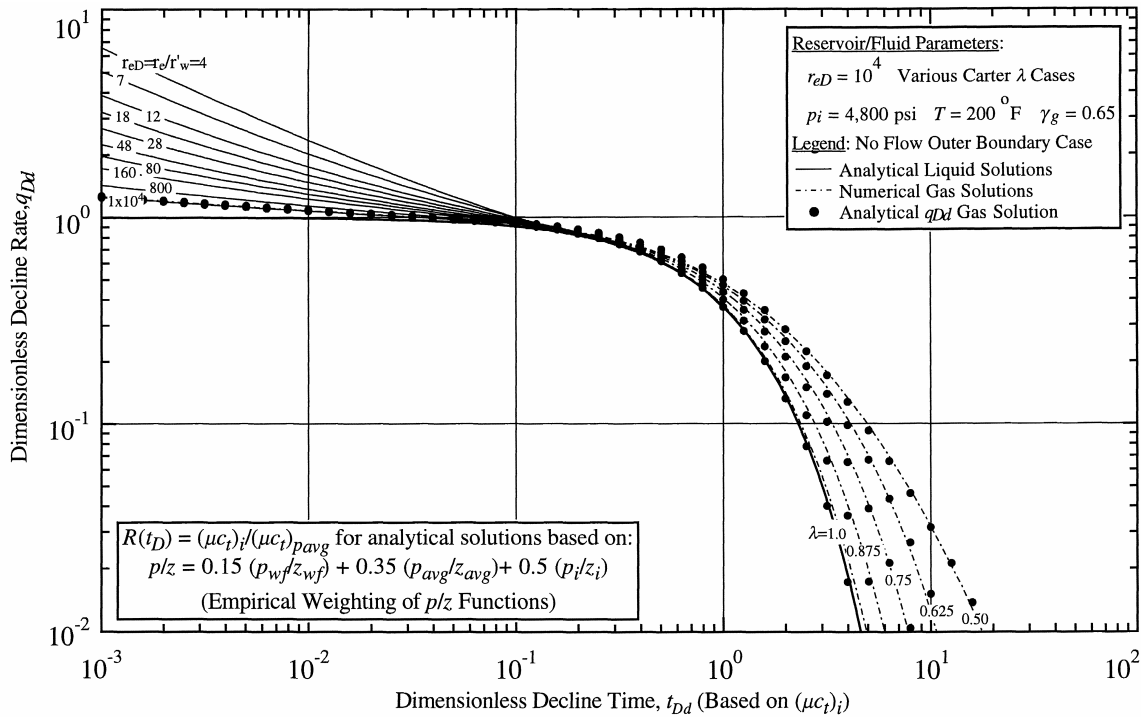


Figure 1.4 — Mireles and Blasingame¹ application of convolution (*i.e.*, superposition of "unit" rate solutions) for constructing the constant rate solution. This is not universal (or even practical) approach — it is an *a posteriori* adjustment using the APA (incorrectly) for the constant pressure case.

Following the ideas above, we will provide a rigorous development of the solution methodology using the same fundamental principles in convolution theory and Laplace transformation. Again, the validity of our results will rely upon the approximation consisting in referencing of the time-dependent viscosity-compressibility product to the average reservoir pressure as a function of time, as computed from material balance. This referencing has physical and mathematical grounds (common theoretical explanation for constant rate and constant pressure problems) that we will discuss.

Numerical simulation will be used to check the validity of the assumption above and more generally of the methodology. It will show whether our approach provides an essentially exact solution for the case of a well producing at a constant bottomhole pressure in a bounded circular reservoir. Finally, we will discuss application of the methodology to more complex cases, and, in particular, to gas flow systems with a time-dependent inner boundary condition (*i.e.*, scheduling of flowing well bottomhole pressure in our context).

Some possible applications of the new approach are as follows:

- Validation of numerical simulator results — assessment of time and space discretization.
- Generation of production rates and well test analysis pressures — especially if a general rate/pressure schedule formulation can be achieved. This would yield a semi-analytical "reservoir simulator."
- Computation of pressure distributions at any time given a prescribed rate history.
- Application to injection/gas displacement problems.

Advantages over alternative methods:

- Numerical Simulator: In case of a constant production rate the solution is robust and direct (it can be evaluated at any time), and has no temporal or spatial discretization (as shown by Mireles and Blasingame¹). For the case of constant wellbore pressure production, the solution is robust and requires only minor temporal discretization. In addition, the constant wellbore pressure solution is competitively fast compared to numerical simulation — and we believe future implementation of this solution may approach the "instantaneous" speed of the constant rate solution. By comparison, numerical simulation solutions must be calibrated in terms of spatial and temporal discretizations.
- Other Approaches: The Average Pressure Approximation (APA) is applicable for a wider range of pressures compared to the p - and p^2 -methods which have very limited validity. In addition, the APA approach is direct and non-iterative, as compared to iterative pseudopressure-pseudotime approach.

CHAPTER II
DEVELOPMENT OF AN ANALYTICAL PRESSURE SOLUTION
FOR THE CASE OF A CONSTANT PRESSURE
INNER BOUNDARY CONDITION

2.1 General Approach

In this work we consider a non-linear parabolic partial differential equation of the following form:

$$\nabla^2 y = \beta(y) \frac{\partial y}{\partial t} \dots\dots\dots (2.1)$$

We show that such an equation effectively describes the flow of real (compressible) gases through porous media. Whereas similar linear equations ($\beta(y) \equiv \text{constant}$) are readily solved using the Laplace transformation, in our case, application of the Laplace transformation is subject to reconstructing the right-hand side of Eq. 2.1 in a more suitable form.

Since y is a function of both spatial and temporal variables and $\beta(y)$ is a composite function, it is necessarily a function of spatial and temporal variables. *Considering spatial variables as independent*, we can write:

$$\beta(t) \frac{\partial y}{\partial t}(t) = \int_0^t \frac{\partial y}{\partial \tau}(\tau) g(t-\tau) d\tau \dots\dots\dots (2.2)$$

We note that the $g(t)$ function must adhere to similar mathematical conditions as $\beta(t)$ (e.g., continuity, boundedness, derivative formulations, etc.). As convolution is commutative, Eq. 2.2 becomes:

$$\beta(t) \frac{\partial y}{\partial t}(t) = g(t) * \frac{\partial y}{\partial t}(t) \text{ (where } * \text{ represents the convolution operation)} \dots\dots\dots (2.3)$$

Another well-known property of the convolution — the Laplace transform of the convolution of two functions is the product of the Laplace transforms of the functions — gives:

$$\mathcal{L}\left[g * \frac{\partial y}{\partial t}\right] = \mathcal{L}[g] \mathcal{L}\left[\frac{\partial y}{\partial t}\right] \dots\dots\dots (2.4)$$

where $\mathcal{L}[g]$ represents non-linearity of the problem.

The new form of Eq. 2.1 is given as:

$$\nabla^2 y = g(t) * \frac{\partial y}{\partial t}(t) \dots\dots\dots (2.5)$$

where y , its temporal derivative and g are actually functions of *both spatial and temporal variables*.

Taking the Laplace transform with respect to time we obtain:

$$\nabla^2 \bar{y}(u) = \mathcal{L}[g(t)] [u\bar{y}(u) - y(t=0)] \quad (u \text{ is the Laplace transform parameter}) \dots\dots\dots (2.6)$$

Coupled with appropriate boundary conditions Eq. 2.6 allows a solution. Obviously, the solution will depend on $\mathcal{L}[g]$. If we can then calculate g for every position in space and time (or $\mathcal{L}[g]$ for every position in space and u) within the region of interest, the Laplace domain solution of Eq. 2.1 will be constructed.

The primary value of this work is that a direct (non-iterative) method of calculating the g -function is proposed (and validated). Moreover, we show that using an "average (pressure) value" approximation eliminates the dependence of g on spatial variables — *i.e.*, g can be taken solely as a function of the average (reservoir) pressure, which is implicitly a function of time.

2.2 Real-Gas Systems

For clarity we will formulate the problem in terms of effective "gas" porosity and neglect residual water compressibility. Also, rock compressibility (*i.e.*, porosity dependence on pressure) will be neglected. It will be evident that our method could be generalized to account for the compressibility effects stated above. Our assumptions are reasonable because residual water and rock compressibility related effects are typically of second order compared to gas expansion (for gas reservoirs) — with the noted exception being abnormally pressured gas reservoirs. Finally, permeability is assumed *constant and independent of pressure*. The interested reader is referred to Appendix A for complete development of this formulation.

Using the following dimensionless groups:

$$t_D = t_{DC} \frac{k}{\phi \mu_i c_i r_w^2} t \dots\dots\dots (2.7)$$

Where t_{DC} equals 0.0002637 or 0.00633 if time is expressed in hours or days, respectively,

$$r_D = \frac{r}{r_w} \dots\dots\dots (2.8)$$

$$m_D = \frac{m_i - m}{m_i - m_{wf}} \dots\dots\dots (2.9)$$

Where the pseudopressure definition (m_D) is characteristic to constant pressure production, and we note that the pseudopressure function is defined as:

$$m = \frac{\mu_i z_i}{p_i} \int_{p_{base}}^p \frac{p}{\mu z} dp \dots\dots\dots (2.10)$$

Combining the continuity equation, Darcy's law, and the definition of isothermal compressibility (for a gas), we obtain the diffusivity equation for real gases in dimensionless form:

$$\frac{1}{r_D} \frac{\partial}{\partial r_D} \left[r_D \frac{\partial m_D}{\partial r_D} \right] = \frac{\mu c}{\mu_i c_i} \frac{\partial m_D}{\partial t_D} \dots\dots\dots (2.11)$$

We note that although the dimensionless form of the pseudopressure for a constant pressure inner boundary condition is defined differently for the case of a constant rate boundary condition (Eq. 1.24) is identical to Eq. 2.11. Obviously, this is because of the linearity of both definitions of dimensionless pressure. The initial and boundary conditions applied to Eq. 2.11 in this work are as follows:

Initial condition (uniform pressure distribution):

$$m_D(t_D = 0) = 0 \dots\dots\dots (2.12)$$

Inner boundary condition (constant well bottomhole pressure production):

$$[m_D]_{r_D=1} = 1 \dots\dots\dots (2.13)$$

Outer boundary condition (no-flow boundary):

$$\left[r_D \frac{dm_D}{dr_D} \right]_{r_D=r_{eD}} = 0 \dots\dots\dots (2.14)$$

We note that the pseudopressure is essentially a potential function, and its gradient is proportional to its flux (per Darcy's law).

Relating Eq. 2.11 to Eq. 2.1 we define:

$$\beta = \frac{\mu c}{\mu_i c_i} \dots\dots\dots (2.15)$$

(β depends on pressure, and thus, in the context of production from a reservoir, β depends on both position and time). Comparing Eq. 2.11 to Eq. 2.2, and using Eq. 2.12 we have:

$$\beta(t_D) \frac{\partial m_D}{\partial t_D}(t_D) = \int_0^{t_D} \frac{\partial m_D}{\partial \tau}(\tau) g(t_D - \tau) d\tau \dots\dots\dots (2.16)$$

Following the logic of the previous section we can write:

$$\frac{d^2 \bar{m}_D(u)}{dr_D^2} + \frac{1}{r_D} \frac{d\bar{m}_D(u)}{dr_D} = [u\bar{m}_D(u) - m_D(t_D = 0)] \bar{g}(u) \dots\dots\dots (2.17)$$

Inner boundary condition becomes:

$$\bar{m}_D = \frac{1}{u} \dots\dots\dots (2.18)$$

and outer boundary condition becomes:

$$\left[r_D \frac{d\bar{m}_D}{dr_D} \right]_{r_D=r_{eD}} = 0 \dots\dots\dots (2.19)$$

One of the most important points of this work is that we can show by induction²⁶⁻²⁷ that:

$$\bar{m}_D(u) = \bar{g}(u) \int_0^\infty p_D(t_D) e^{-u\bar{g}(u)t_D} dt_D \dots\dots\dots (2.20)$$

or

$$\bar{m}_{D,gas}(u) = \bar{g}(u) \bar{m}_D(u\bar{g}(u)) \dots\dots\dots (2.21)$$

where \bar{m}_D is the dimensionless solution in the Laplace domain for the linear (*i.e.*, "liquid" or "slightly compressible") formulation. In this work we construct a solution in analytical form for our boundary conditions. However, in order to implement this formulation we must find a relationship between $\beta(r_D, t_D)$ and $\bar{g}(r_D, u)$.

As noted by Mireles and Blasingame¹ the form of this solution (Eq. 2.21) is *equivalent in form* to the analytical solution developed for the case of a naturally fractured (dual porosity) reservoir.²⁶ In reviewing Eq. 2.21, it is obvious that we obtain the $\bar{g}(r_D, u)$ function independently — this is elegant for the constant rate case, but becomes problematic for the case of production at a constant bottomhole flowing pressure (*i.e.*, we must develop a methodology which computes rate and average reservoir pressure simultaneously). This is discussed in detail in other sections of this thesis.

2.3 Key Relation

As with the work of Mireles and Blasingame,¹ we use the gas material balance to establish a relationship between $\beta(r_D, t_D)$ and $\bar{g}(r_D, u)$. This leads to the APA approach — *i.e.*, referencing to average reservoir pressure:

$$\beta_{\bar{p}} = \frac{\bar{\mu}c}{\mu_i c_i} \dots\dots\dots (2.22)$$

such that dependence of β -function on position is eliminated, and the right-hand side of Eq. 2.11 depends only on time. Appendix B provides the mathematical developments which were required to identify the following relationship given by:

$$q(t_D) = \int_0^{t_D} \left[\frac{q}{\beta_{\bar{p}}}(\tau) \right] g(t_D - \tau) d\tau \dots\dots\dots (2.23)$$

which yields after the Laplace transformation:

$$\mathcal{L}[g(t_D)] \equiv \bar{g}(u) = \frac{\mathcal{L}[q(t_D)]}{\mathcal{L}\left[\frac{q}{\beta_{\bar{p}}}(t_D)\right]} \dots\dots\dots (2.24)$$

Note that, by construction, our expression for $\bar{g}(u)$ given by Eq. 2.24 contains the defining expression for a constant rate boundary condition (Eq. 1.26) as a particular case. Further, as Eq. 2.24 contains the rate, *the strategies proposed by Mireles and Blasingame¹ to calculate $\bar{g}(u)$ are not applicable.*

In the case addressed by Mireles and Blasingame the average reservoir pressure (and therefore $\beta_{\bar{p}}$) can be directly obtained because the rate is known. In our case — *i.e.*, the constant pressure inner boundary condition, *we must calculate $\bar{g}(u)$ using temporal discretization.* In Chapter 3 we present a strategy for obtaining $\bar{g}(u)$ and, thus, enabling us to apply Eq. 2.21.

In the following section we discuss our choice of algorithms for Laplace and inverse Laplace transformations.

2.4 Laplace and Inverse Laplace Transformations

For the case of a constant production rate Eq. 2.24 is reduced to:

$$\mathcal{L}[g(t_D)] \equiv \bar{g}(u) = \frac{1}{u} \frac{1}{\bar{R}_{\bar{p}}(u)} \dots\dots\dots (2.25)$$

where

$$\bar{R}_{\bar{p}}(u) = \mathcal{L}[R_{\bar{p}}(t_D)] = \mathcal{L}\left[\frac{1}{\beta_{\bar{p}}}(t_D)\right] \dots\dots\dots (2.26)$$

Mireles and Blasingame¹ developed two strategies for obtaining the $\bar{R}_{\bar{p}}(u)$ function — functional (its advantage consisting in an analytical Laplace transformation) and numerical (based on discrete values). Mireles and Blasingame used exponential, polynomial, and hyperbolic relations within the functional strategy. After an extensive study of behavior of the $R_{\bar{p}}(t_D)$ function with variations in temperature, initial pressure, and gas specific gravity (or composition) it appears that the functional models mentioned above have serious limitations — for example, these functional forms do not always accurately model the non-linear behavior for a wide range of conditions. In other words, we need a more general mechanism.

As we showed in the previous section, the constant pressure production calculation of $\bar{g}(u)$ is more complex, *and it is absolutely clear that functional models are not applicable.* Thus, we will use numerical transformations of these data functions for use in the Laplace domain. We can transform data into the Laplace domain using one of existing algorithms: Rouboutsos and Stewart,²⁴ Blasingame, *et al.*,²⁸

interpolating functions. As Mireles and Blasingame¹ we chose to use the Rouboutsos and Stewart algorithm because of its ease of implementation. We verified for our cases that the Rouboutsos and Stewart algorithm combined with carefully chosen timesteps yields accurate and consistent results. Mireles and Blasingame¹ noticed that the initial data point was always inverted incorrectly. We analyzed this issue and proposed a modification to the Rouboutsos and Stewart algorithm that eliminates this error. In Appendix C we provide a discussion of some aspects of the numerical Laplace transformation as well as the modified implementation of the Rouboutsos and Stewart algorithm.

To numerically compute the inverse Laplace transforms (to construct real-domain solutions) we use the de Hoog, *et al.*²⁹ quotient difference method with accelerated convergence for the continued fraction expansion. The Stehfest²⁵ algorithm which is very popular in petroleum engineering (because it only considers small samples of the Laplace domain solution) was also considered. However, as Rouboutsos and Stewart noted:

It should be noted that the Stehfest inversion algorithm is strictly limited to continuous functions and it will fail drastically if, for example, steps are present in the rate schedule.

Indeed, for discontinuous functions (like step-rate or pressure schedules) Fourier-type inversion algorithms perform better than sampling algorithms of the Stehfest-type. Our choice of the de Hoog, *et al.* algorithm was determined due to our anticipation of application to a problems with time-dependent inner boundary condition (arbitrary schedules of flowing well bottomhole pressure).

CHAPTER III

**VALIDATION OF THE PROPOSED CONSTANT PRESSURE SOLUTION
AND THE AVERAGE PRESSURE APPROXIMATION:
A DIRECT PROCEDURE FOR PERFORMANCE PREDICTION**

We propose a twofold approach. Since Eq. 2.24 contains rate, we will generate the rate history for a particular reservoir system using a finite-difference simulator, then calculate the average pressure versus time relationship using gas material balance, then calculate $\beta_{\bar{p}}$ versus time, and finally obtain $\bar{g}(u)$. This will allow us to calculate the real-domain solution of Eq. 2.11 according to Eq. 2.21, specifically as a validation, we generate profiles of dimensionless pseudopressure versus radius for different times. The goal is to compare these profiles to those generated by a numerical simulator for exactly the same production schedules.

Second, suppose that computed pseudopressure profiles coincide. Then our conclusion is that if we can generate the correct rate history, then the computed pressure profiles are also correct. *In other words, achieving the correct pressure profiles with our computational approach would constitute a necessary condition of correctness for the proposed rate calculation.* As such, we concentrate on the computation of the flowrate profiles as a mechanism to validate our method — again, we will check both the computed rate profiles and the computed pressure profiles against results from numerical simulation.

Both parts of the validation computations are implemented in *Matlab*³⁰ — which, due to its precision and structure, is probably the best environment for our numerical calculations. We performed numerous checks for accuracy, and we optimized for the speed of execution. In Appendix D we provide a discussion of these algorithms and make suggestions for the practical implementation of this methodology.

The most effective mechanism to validate our method (and, in particular, the APA concept) lies in comparison of results to those of a numerical simulator. We chose an in-house simulator known as *Gassim*.³¹ This module has a long development and validation history and we systematically tested for its convergence by refining spatial and temporal discretizations. We refer to *Gassim* as the *numerical simulator* for the remainder of this thesis.

3.1 Verification Based on Numerical Simulator Outputs — Verification of Pressure Profiles

Using the numerical simulator for a known reservoir configuration, we can generate the rate and average pressure history corresponding to a particular constant pressure inner boundary condition. Using these rate and pressure histories, and Eqs. 2.21 and 2.24, we compute the solution to the diffusivity equation for the case of a gas well being produced at a constant bottomhole flowing pressure. The semi-analytical

solution provides us with pressure profiles in the reservoir for different times, which we then compare to the pressure profiles generated by the finite-difference simulator.

Note that instead of using the average reservoir pressure history generated by the simulator we can generate this history from the rate history and the material balance equation. We would expect these profiles to be essentially equal — and all of our test cases confirmed this hypothesis.

The reservoir-production system described in **Table 3.1** is used to test the new semi-analytical solution, where we have generated pseudopressure profiles based on these properties. **Figs. 3.1 and 3.2** show very good matches between the dimensionless pseudopressure functions generated by our method and by the numerical simulator. In **Fig. 3.2** we note that the profiles generated by the numerical simulator tend towards the profiles generated by our method when a finer temporal discretization is used in the numerical simulator.

Table 3.1 — System Parameters for Pressure Profiles Validation Cases.

Reservoir properties:

$$\begin{aligned} k &= 50 \text{ md} \\ \phi &= 0.15 \\ h &= 50 \text{ ft} \\ r_w &= 0.25 \text{ ft} \\ r_e &= 1200 \text{ ft} \end{aligned}$$

Gas properties:

$$\begin{aligned} T &= 200^\circ\text{F} \\ \gamma &= 0.7 \text{ (air=1)} \\ p_i &= 3000 \text{ psia} \end{aligned}$$

Production parameters:

$$p_{wf} = 2500 \text{ psia}$$

We note that we do not provide values for comparison for $r_D < 2.04$ in **Fig. 3.1** since this value corresponds to the center of the inner-most gridblock in the spatial discretization implemented in the numerical simulator. Nevertheless, we note that for r_D tending to 1 (wellbore surface), m_D calculated by our method tends to the correct value which is (of course) 1 (by definition).

We do not present an exhaustive comparison in this section, but rather, we prefer to do so in the next section because the correctness of pressure profiles (shown in this section) is a necessary condition for the correctness of rates (shown in the next section).

On the other hand, our prior statement regarding a necessary condition is *empirical* if we base this statement only using comparison of numerical results. The question as to how can we demonstrate this statement theoretically? This is one direction for improving this work. An idea for such a demonstration is as follows — since the rate history is correct, then at every time the pressure and its gradient at the

wellbore should be correct (if the deliverability equation is given by Darcy's law), we can then construct a suite of concentric cylinders and propagate the constructed pressure profile towards higher r_D -values.

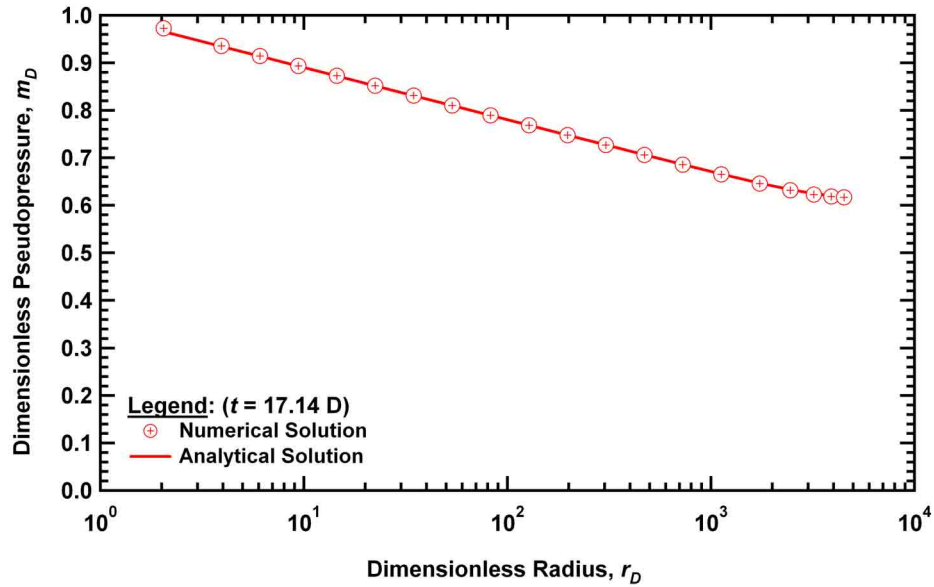


Figure 3.1 — Dimensionless pseudopressure profile at $t = 17.14 D$ for the reservoir system presented in Table 3.1.

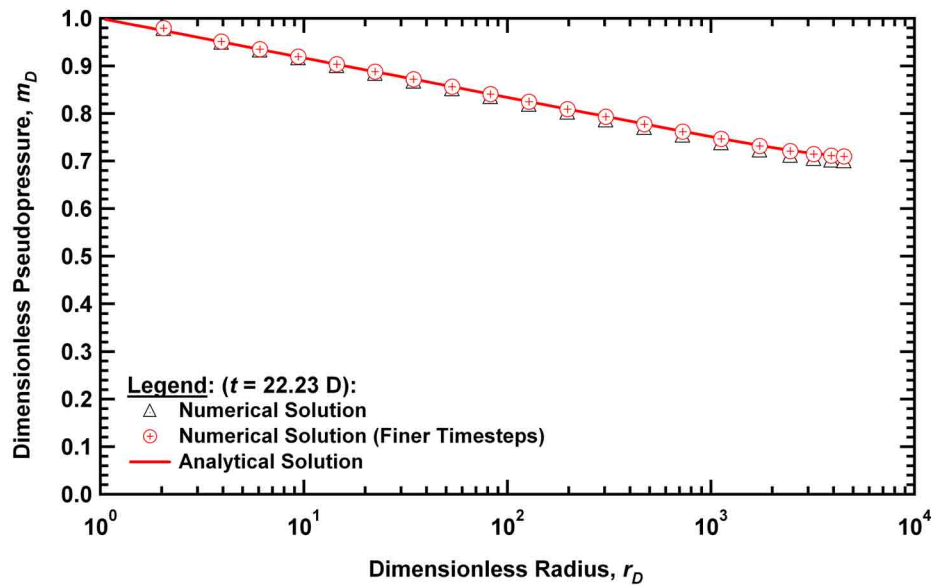


Figure 3.2 — Dimensionless pseudopressure profile at $t = 22.23 D$ for the reservoir system presented in Table 3.1.

3.2 Forward Modeling (Performance Prediction)

We now consider that the rate history is not available and we want to use our approach to *predict both rates and reservoir pressure profiles at any time* — what we will call *performance prediction*. To achieve this goal we obviously need to couple our pressure solution with a deliverability equation (or possibly deliverability equations), since there will be more than one flow regime encountered during the production. We note that only Darcy's law is universally valid, but we will test Darcy's law as well as other formulations for robustness and correctness.

In order to properly calculate flowrates during the transient period (as well as during pseudosteady-state (PSS) period), we will use the deliverability equation given by Darcy's law (radial geometry):

$$q = \frac{1}{25.148} \frac{kh}{B\mu} r \frac{\partial p}{\partial r} \dots\dots\dots (3.1)$$

In Eq. 3.1, the thermodynamic properties and pressure gradient are calculated at the wellbore surface (*i.e.*, $r_D = 1$). In particular, the gas FVF (B) and the gas viscosity (μ) are calculated at p_{wf} .

The proposed general procedure is direct and consists of the following steps:

1. Timesteps are chosen so that the rate is assumed constant during a particular time interval.
2. The average reservoir pressure is calculated at the *end of the timestep* using the gas material balance equation.
3. The computed average reservoir pressure is used to estimate the non-linear term ($\beta_{\bar{p}}$), and, using the $\beta_{\bar{p}}$ history and the rate history (computed prior), we can obtain $\bar{g}(u)$ using Eq. 2.24.
4. We then generate a pressure profile in the vicinity of the wellbore surface and use this to calculate the pressure gradient term required in Darcy's law (the near-well gradient is estimated using a finite-difference approximation).
5. The timestep is updated and the procedure is repeated as described above.

Attention should be paid when calculating the very first rate (at $t = 0$) as this is the moment where a discontinuity in pressure exists. Obviously, there will not be an ζ such that for all $r_D < 1 + \zeta$ the pressure profile will be essentially linear (if we use a first-order finite-difference formulation) — for r_D tending to 1 the rate will tend to infinity. This issue is resolved in a practical sense by using a larger argument difference for the first rate calculation, or by using a very small first timestep (for the case of approximating the gradient at the first timestep, we recommend a difference of $\sim 2-5 r_D$, whereas for subsequent timesteps, a difference smaller than $\sim 0.02 r_D$ gives excellent results).

We test our method on two sets of reservoir properties. Following Mireles and Blasingame¹ we will use fluid properties given in **Table 3.2** because they represent a typical set of conditions.

Table 3.2 — Gas Properties.

$$\begin{aligned} T &= 200^{\circ}\text{F} \\ \gamma &= 0.7 \text{ (air=1)} \\ p_i &= 5000 \text{ psia} \end{aligned}$$

As to reservoir properties we use the Mireles and Blasingame¹ high porosity/low permeability set (**Table 3.3**) as well as a lower porosity/higher permeability set (**Table 3.4**). The difference between these two sets is that dimensionless time as defined by Eq. 2.7 is 100 times "slower" for the reservoir properties given in **Table 3.3**, compared to **Table 3.4**. Besides, the equation for radius of investigation given by:

$$r_{inv} = 0.032 \sqrt{\frac{24kt}{\phi\mu c}} \dots\dots\dots (3.2)$$

shows that the transient period for Mireles and Blasingame set will be substantially longer — compare

$$r_{inv} = 30.98\sqrt{t} \dots\dots\dots (3.3)$$

to

$$r_{inv} = 309.8\sqrt{t} \dots\dots\dots (3.4)$$

In Eqs. 3.3 and 3.4 we estimated the thermodynamic properties at $p_i = 5000$ psia (same value is used for all "rate" validation cases).

Table 3.3 — Mireles and Blasingame Set of Reservoir Properties (Type 1).

$$\begin{aligned} k &= 1 \text{ md} \\ \phi &= 0.3 \\ h &= 30 \text{ ft} \\ r_w &= 0.25 \text{ ft} \end{aligned}$$

Table 3.4 — Reservoir Properties (Type 2).

$$\begin{aligned} k &= 50 \text{ md} \\ \phi &= 0.15 \\ h &= 50 \text{ ft} \\ r_w &= 0.25 \text{ ft} \end{aligned}$$

For both sets we will study three reservoir sizes: $r_{eD} = 10^2, 10^3, 10^4$. Each reservoir will be produced at high, low and intermediate rates (**Table 3.5**). This scheme (5 drawdowns (p_{wf}/p_i), 3 reservoir sizes, and 2 types of reservoir) gives us 30 cases.

Table 3.5 — Flowing Bottomhole Pressure Schedules (Used in Performance Prediction).

Case	Flowing Bottomhole Pressure (psia)	Ratio p_{wf}/p_i (fraction)
Low	4900	0.98
Intermediate 1	4000	0.8
Intermediate 2	2500	0.5
Intermediate 3	1000	0.8
High	100	0.02

Time and rate are made "dimensionless" using the "dimensionless decline time" and "dimensionless decline rate" definitions proposed by Fetkovich¹⁹ and modified by Carter:³²

$$t_{Dd} = 0.00633 \frac{k}{\phi \mu_i c_i r_w^2} \frac{1}{\frac{1}{2} \left[\left[\frac{r_e}{r_w} \right]^2 - 1 \right] \left[\ln \left[\frac{r_e}{r_w} \right] - \frac{1}{2} \right]} t \dots\dots\dots (3.5)$$

$$q_{Dd} = 25.148 \frac{\mu B}{kh(m_i - m_{wf})} \left[\ln \left[\frac{r_e}{r_w} \right] - \frac{1}{2} \right] q(t) \dots\dots\dots (3.6)$$

Fetkovich¹⁹ and Carter³² showed that using the definitions given above, the rate histories for different types of reservoir properties (Type 1 and 2 in our context) but the same production constraint will "collapse" to a common trend for all times if the reservoirs are the same size. This is another validation criterion for our approach, as this "collapse" of solutions will be true only if our method is fundamentally correct. Without understanding how the APA works, we cannot expect these solutions to collapse *a priori*. Of course, our curves must also coincide with corresponding numerical simulator results.

Let us underscore another important property of the Fetkovich-Carter coordinates. For the same reservoir fluid and initial pressure, the flowrates for different cases (sizes and pressure drawdowns) plotted in these coordinates differ only by the reservoir size (the pressure drawdowns are irrelevant) during transient flow and only by pressure drawdown (reservoir sizes are irrelevant) during boundary-dominated flow.

We typically predict performance until q_{Dd} reaches values of order of 10^{-3} - 10^{-4} , which corresponds to a gas flowrate on the order of 10 MSCF/D for reservoir Type 2 cases. An extreme example for a reservoir Type 2 case is a size of $10^4 r_w$ produced at $p_{wf}=100$ psia (for comparison, the initial rate of such a system is of order of 100,000 MSCF/D).

As would be expected, the real time needed for the flowrate to decrease to such small values depends on the reservoir properties. For $r_{eD} = 10^4$ and an extreme drawdown ($p_{wf}=100$ psia), the time needed for a reservoir of Type 1 is of order of 50,000 days, while for a reservoir of Type 2 depletion to the same state would occur in only 500 days.

This approach (based on Eq. 3.1) is computationally intense and more difficult to implement than ones based on PSS-type deliverability equations (discussed in the following section and in Appendix D). However the application of Eq. 3.1 yields excellent results (**Figs. 3.3-3.7**), and production curves for the different reservoir types coincide almost identically with the corresponding numerical simulator results — and thus with each other provided they were generated for the same reservoir size and production constraint (for clarity in these graphics, we plot only a single trend for either reservoir type). The APA seems to be a uniquely correlative concept as it allows us to correctly estimate the near-wellbore pressure gradient and subsequently obtain good estimates of the gas production rate.

In **Figs. 3.3-3.5** Arps¹⁸ empirical hyperbolic decline curves (and their limiting cases — exponential and harmonic) are superimposed with the results of numerical simulation and our semi-analytical approach — and we note generally good to excellent matches of the numerical and semi-analytical results (except at very late times where the numerical solution begins to fail). It is interesting to note an essentially exponential decline for production at the lowest drawdown ($p_{wf}=4900$ psia) — recalling what was said in the literature review, we understand this pressure range as a zone of validity of the p -method, that is the gas behaves like a "slightly compressible" fluid. For larger pressure drawdowns we note that the computed solutions (both numerical and semi-analytical) are not hyperbolic — where we note that, in practice, the hyperbolic rate decline model is very popular — particularly for the analysis of gas production data. This observation suggests that the hyperbolic rate relation should not be used as a general model for gas flow behavior at boundary-dominated flow conditions.

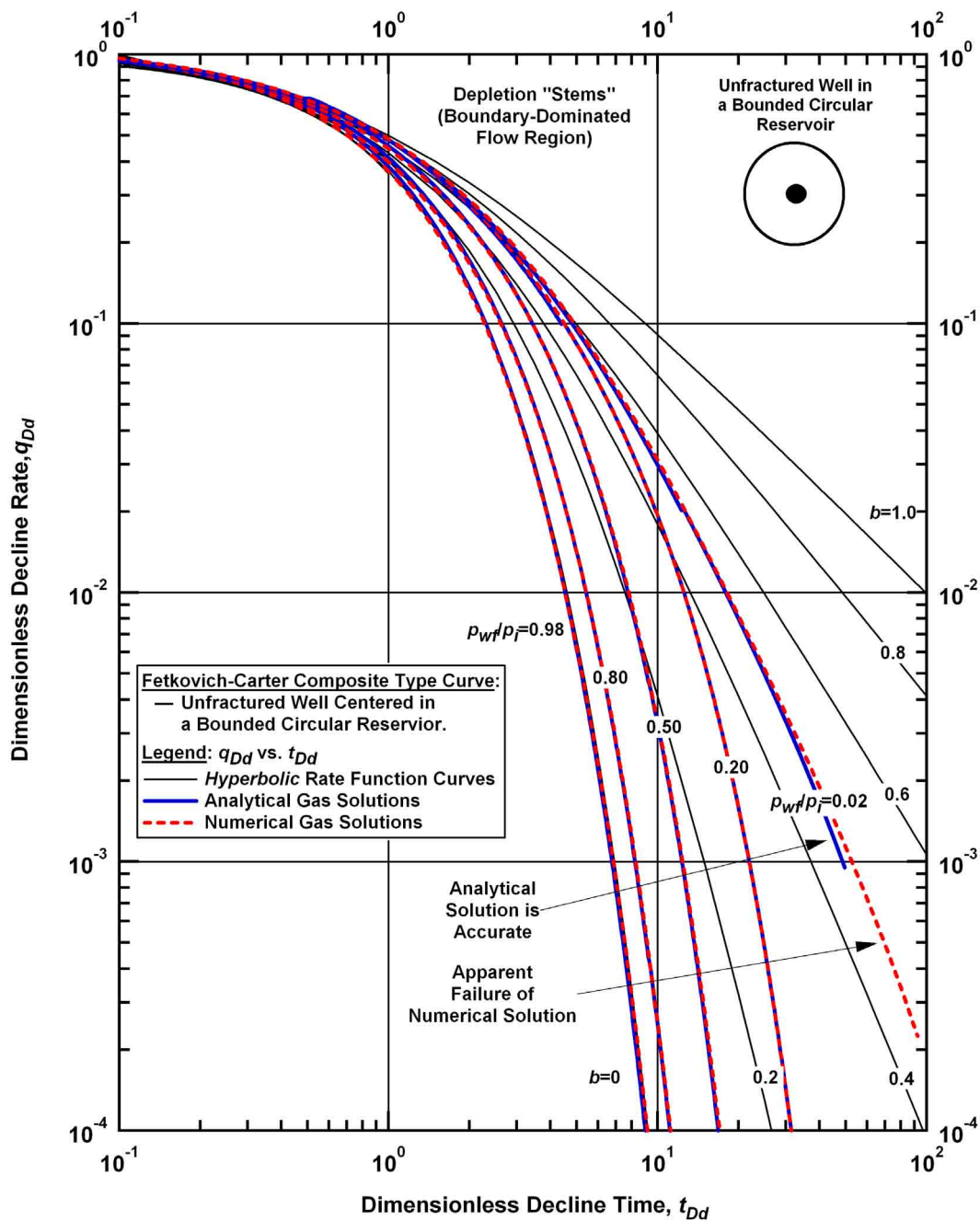


Figure 3.3 — Fetkovich-Carter "composite" rate type curve — zoom view (Type 1 and 2 cases, $r_{eD} = 10^2$).

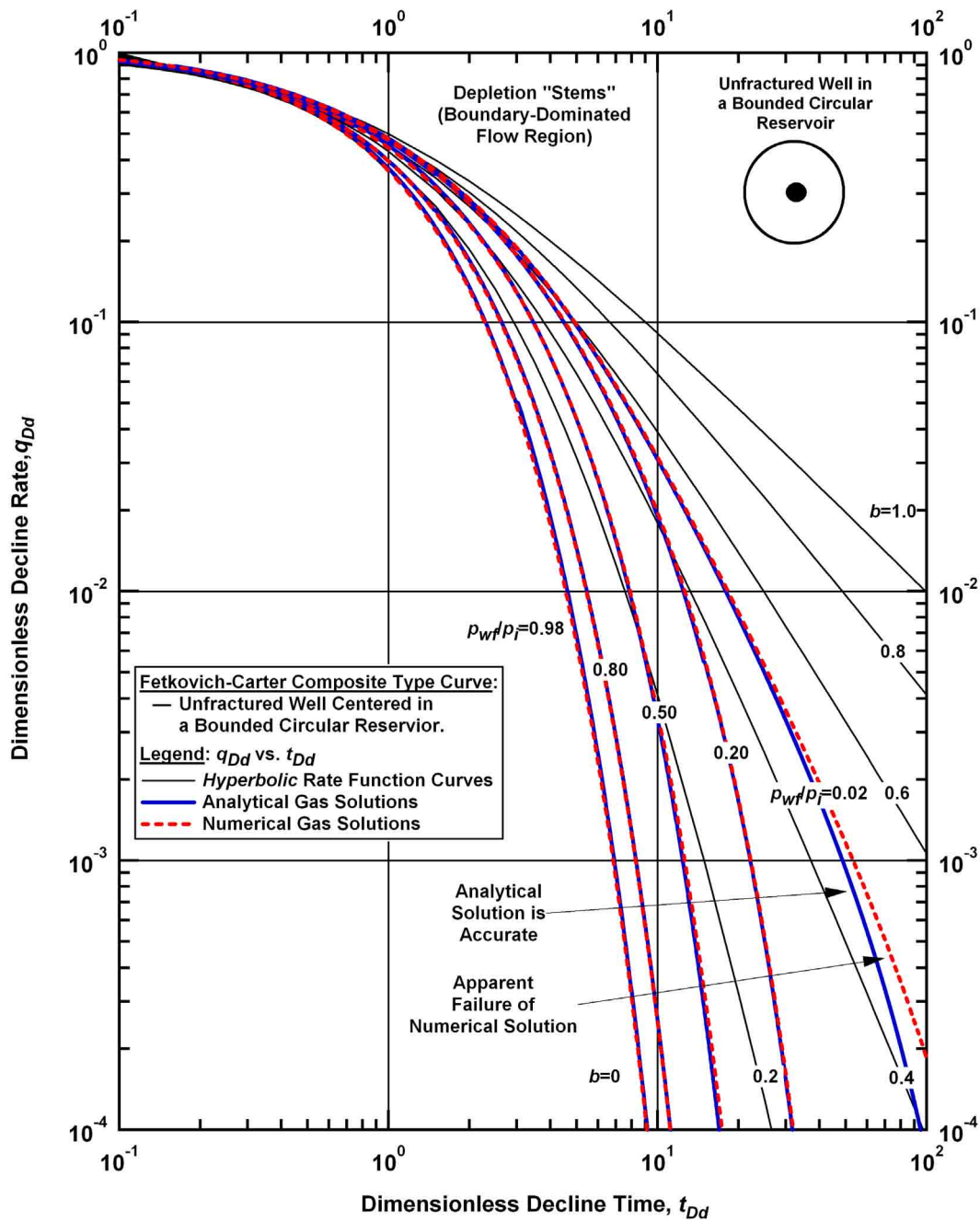


Figure 3.4 — Fetkovich-Carter "composite" rate type curve — zoom view (Type 1 and 2 cases, $r_{eD} = 10^3$).

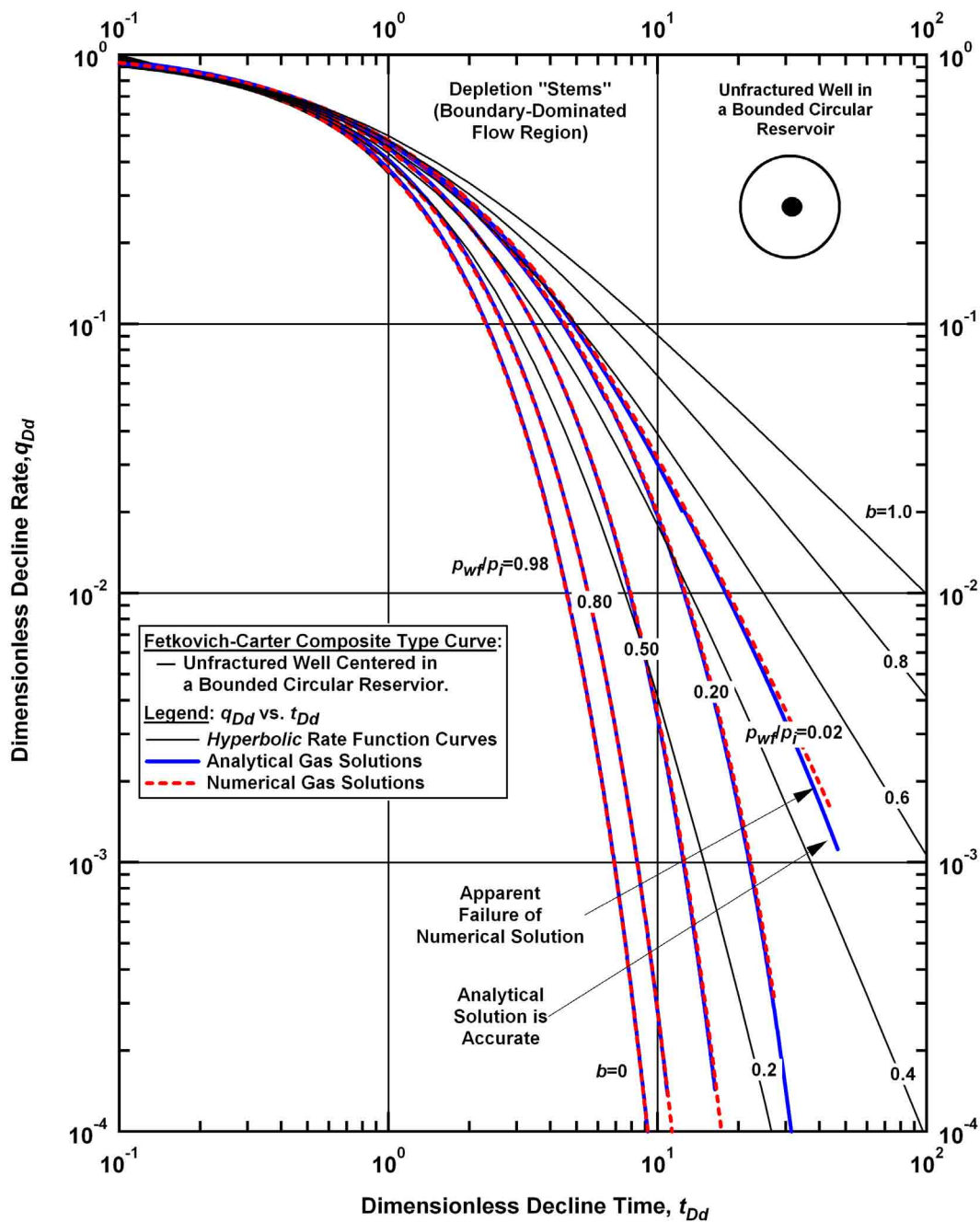


Figure 3.5 — Fetkovich-Carter "composite" rate type curve — zoom view (Type 1 and 2 cases, $r_{eD} = 10^4$).

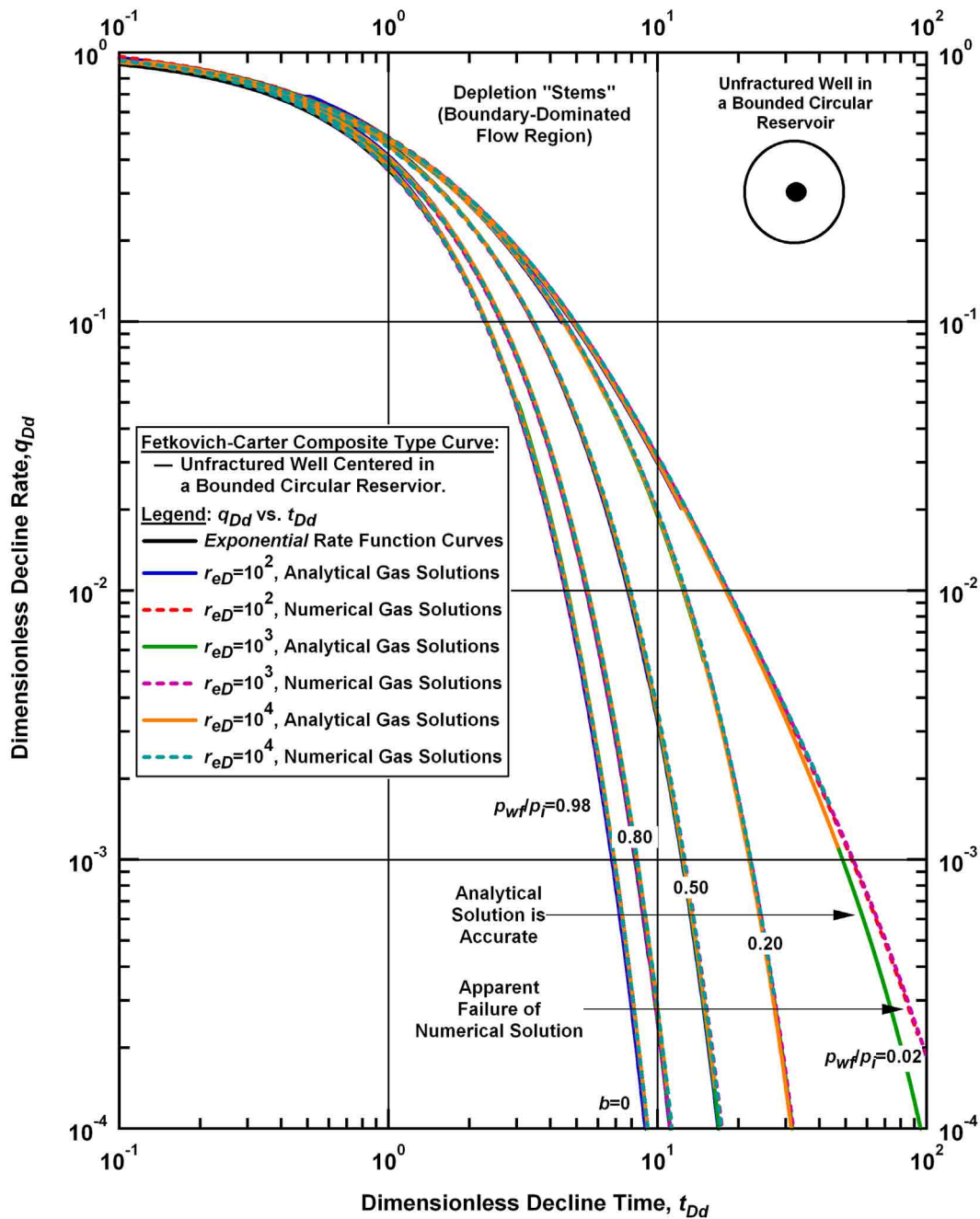


Figure 3.6 — Fetkovich-Carter "composite" rate type curve — zoom view (Type 1 and 2 cases, superposition of $r_{eD} = 10^2, 10^3, 10^4$).

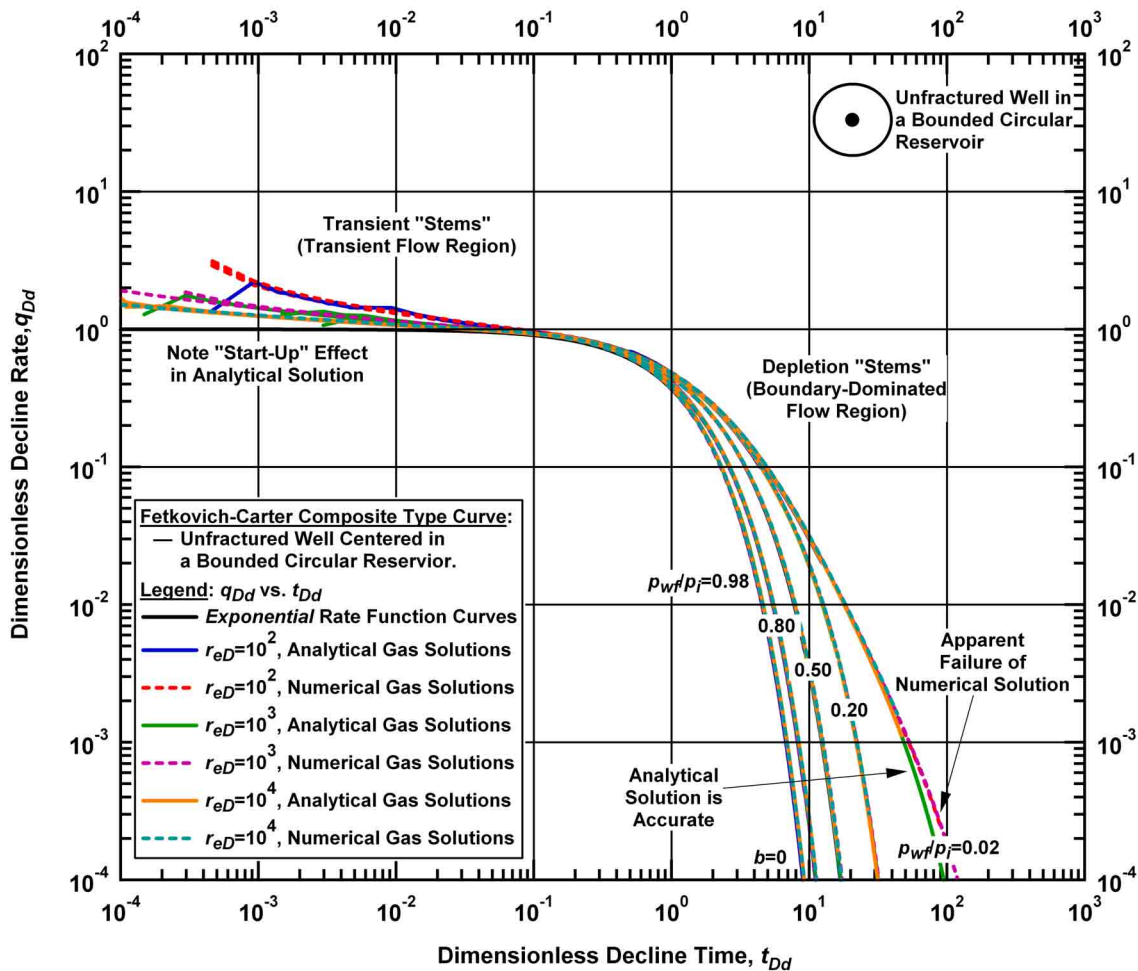


Figure 3.7 — Fetkovich-Carter "composite" rate type curve — global view (Type 1 and 2 cases, superposition of $r_{eD} = 10^2, 10^3, 10^4$).

In **Fig. 3.6** we "zoom in" on large t_{Dd} region (where reservoir size is irrelevant), and we note, as would be expected, that the numerical and semi-analytical production trends differ only by the pressure drawdown. **Figure 3.7** shows the rate performance for all production times (*i.e.*, all t_{Dd}). We note, in particular, (as expected) that the numerical and semi-analytical production trends differ only by the reservoir size (*i.e.*, r_e/r_w) during the early (transient) production period. We note that during transition from transient to boundary-dominated flow that all of the production trends yield an "apparent" exponential decline regime. The basis for this behavior is that, during transient flow, the μc -product does not vary significantly, and we obtain "liquid"-like performance (*i.e.*, the non-linearity does not significantly affect the solution, and the "linear" (or liquid) flow solution is approximately valid (which in this case is the exponential decline)).

In **Figs. 3.3-3.7** we also observe an apparent failure of numerical solution for the case of extreme drawdown ($p_{wf}/p_i = 0.02$). This is due to a limitation on number of timesteps in the numerical simulator that we used. Because of such limitation we could not use appropriately small timesteps for late times where average pressure was small (extreme drawdown). The impact of timestep size on our semi-analytical method is explained in the next paragraph. The impact on the numerical simulator can be explained in similar manner.

The μc product values can be divided into two zones according to the rate of its change with pressure (first derivative): high pressure, or "slow," and low pressure, or "fast," (**Fig. 1.2**). We know that the rate decreases with time. Thus, if our timestep is too large, then we overestimate cumulative production at the end of the timestep; consequently, average pressure is underestimated. The difference between "slow" and "fast" regions is that in the former a small error in the computed average pressure will result in a small error in the β -function (normalized μc product), whereas in the latter case (low pressure) the error in β -function will be amplified. If we consider this effect in isolation, then we should modify the timestep size as a function of the slope of the μc product versus pressure. **Figure 3.8** shows that using finer timesteps during late times yields a more accurate solution.

We empirically found that in case of extreme drawdowns, keeping the timestep essentially constant (and very small) yields the most accurate results (as would be expected). But again, this is only required if we enter the range of very low pressures — in all other cases the timesteps can be increased with production time.

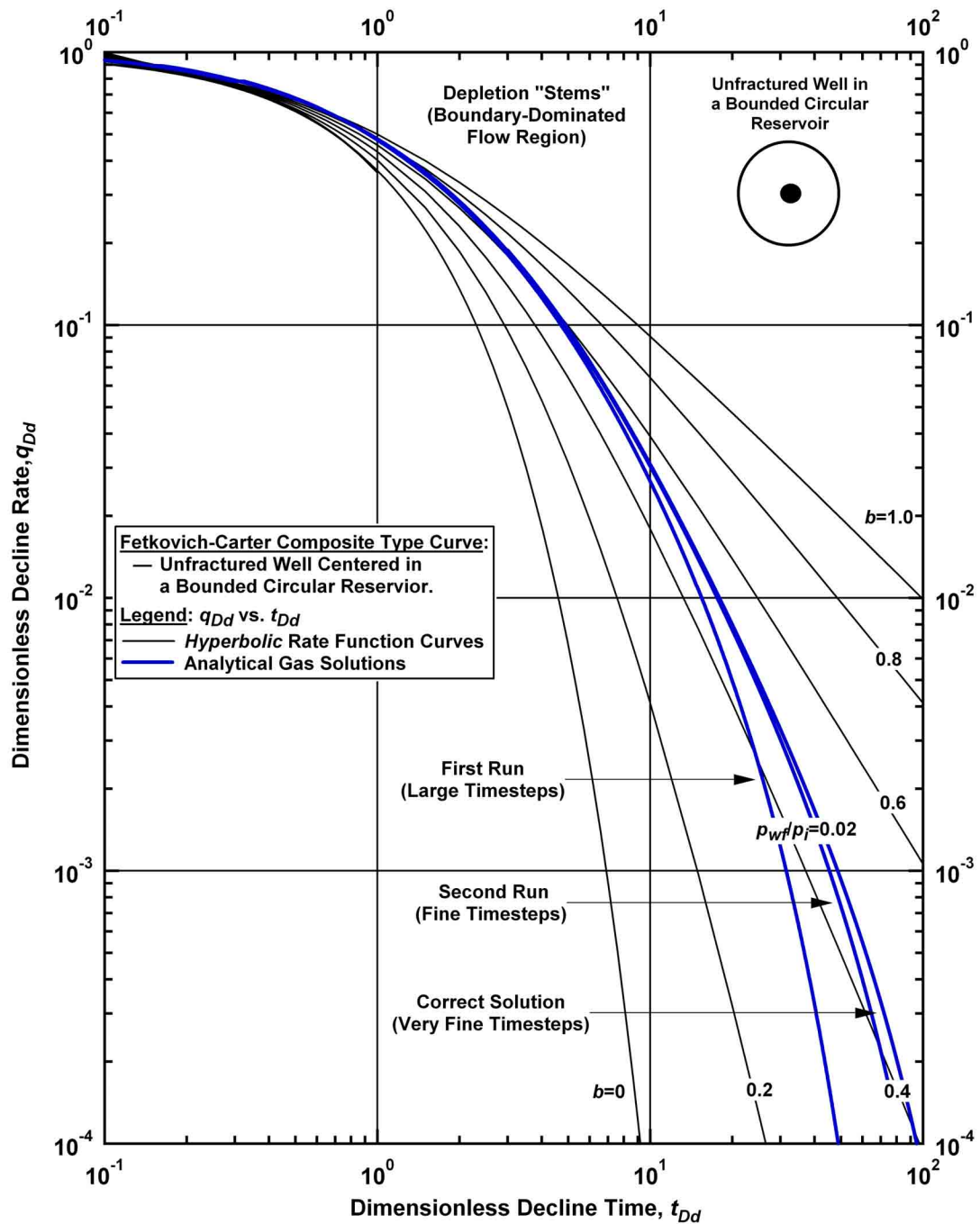


Figure 3.8 — Fetkovich-Carter "composite" rate type curve — zoom view of timestep-related convergence (Type 1 and 2 cases, $r_{eD} = 10^3$).

Finally, we note the "start-up" effect (**Fig. 3.7**) caused by the discontinuity at $t = 0$ of the pressure distribution. Regardless of the case, the solution becomes correct in one or two timesteps.

Since the thermodynamic properties for gases with different gravities and different temperatures often look similar (in the sense of pressure dependence), we affirm that our method will work for any cases of gas properties and temperatures.

The very slight deviation between flowrates predicted by the numerical simulator and our method is a topic for further study. We note that the effect of such deviations is trivial in a practical sense (all numerical and semi-analytical solutions agree (with the noted exception of the numerical solution computed at very late times for cases of extreme drawdowns (where this case has problems of its own))). To assess the mechanistic differences in the numerical and semi-analytical solutions, we suggest that three avenues of investigation be considered:

- The intrinsic error related to the APA (Appendix B),
- Accuracy of numerical procedures (Appendix D), and (possibly)
- Different thermodynamic correlations.

The issue of thermodynamic correlations/properties warrants further orientation — in fact, in our work we use the same correlations for all activities — the Dranchuk and Abou-Kassem³³ correlation for z -factor (and gas compressibility) and Lee, Gonzalez, Eakin³⁴ correlation for gas viscosity. We note that we used the pseudocritical correlation from Piper, McCain, and Corredor³⁵ for the semi-analytical solution and the correlation from Sutton³⁶ for the numerical simulations. However, we must note that since all of our results are presented as "dimensionless" (*e.g.*, rate comparisons) or in terms of "normalized" pseudo-pressure (*e.g.*, pressure distribution plots), so this matter is trivial at best — but does warrant acknowledgement and future consideration.

3.3 Alternative Deliverability Equations

Let us assume that the pseudosteady-state (PSS) deliverability equation is valid for our purposes:

$$q = \frac{0.703kh(\bar{p}^2 - p_{wf}^2)}{(\mu z)_{p_{wf}} (T + 459.67) \left[\ln \left[\frac{r_e}{r_w} \right] - \frac{3}{4} \right]} \dots\dots\dots (3.7)$$

Timesteps are chosen such that the average reservoir pressure can be assumed to be constant during a particular timestep interval. Thus, for the very first timestep, we can assume average reservoir pressure to be equal to the initial pressure. Eq. 3.7 will yield the corresponding rate. Then, using the rate and average reservoir pressure we can calculate $\bar{g}(u)$ according to Eq. 2.24 and finally generate the pressure profile for this timestep. Again, we can calculate the average pressure at the end of the timestep in two ways —

either using the rate and material balance equation, or by calculating the average reservoir pressure from the generated pressure profile.

A "deliverability" equation which uses the average reservoir pressure profile (*e.g.*, Eq. 3.7) results in a smaller computational burden because we eliminate the need for the Laplace domain computations at every timestep — and only perform the Laplace domain computations when we want to generate a pressure profile (see Appendix D). However, such deliverability equations are only valid during pseudosteady-state (or PSS) flow regime.

Figures 3.9 compares the rate histories generated using Darcy's law (Eq. 3.1) and the PSS relation given by Eq. 3.7. In **Fig. 3.10** we compare the pressure profiles generated using our methodology based on Darcy and PSS rate histories above — and we note that Darcy's law is the more rigorous approach. The reservoir system we used is of Type 2 ($r_{eD} = 10^4$ and $p_{wf} = 4500$ psia). We note in **Fig. 3.11** that cumulative error in pressure profiles decreases with time. *However, this cumulative error is unique due to the fact that the PSS deliverability equation does not correctly predict rate during transient period.* If we elected to use Darcy's law during the transient flow period, and then switch to the PSS equation, the error will be eliminated.

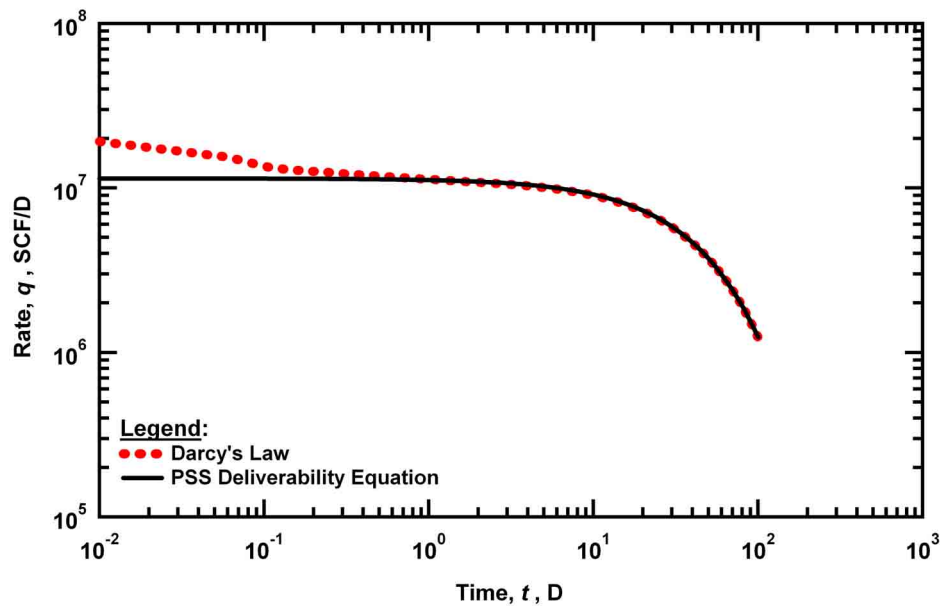


Figure 3.9 — Comparison of rates predicted by coupling our solution with Darcy's law and PSS deliverability equation.

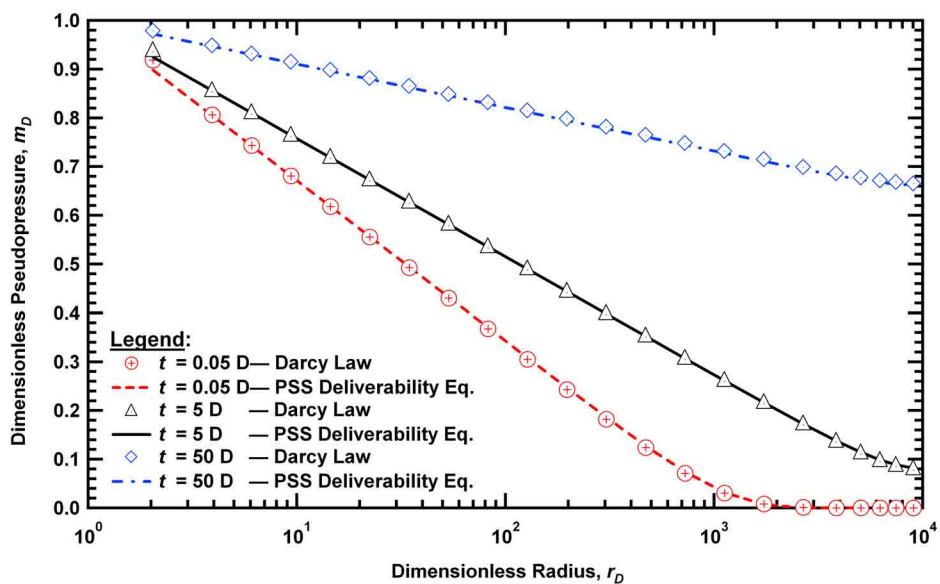


Figure 3.10 — Semilog comparison of pressure profiles predicted by coupling our solution with Darcy's law and the PSS deliverability equation.

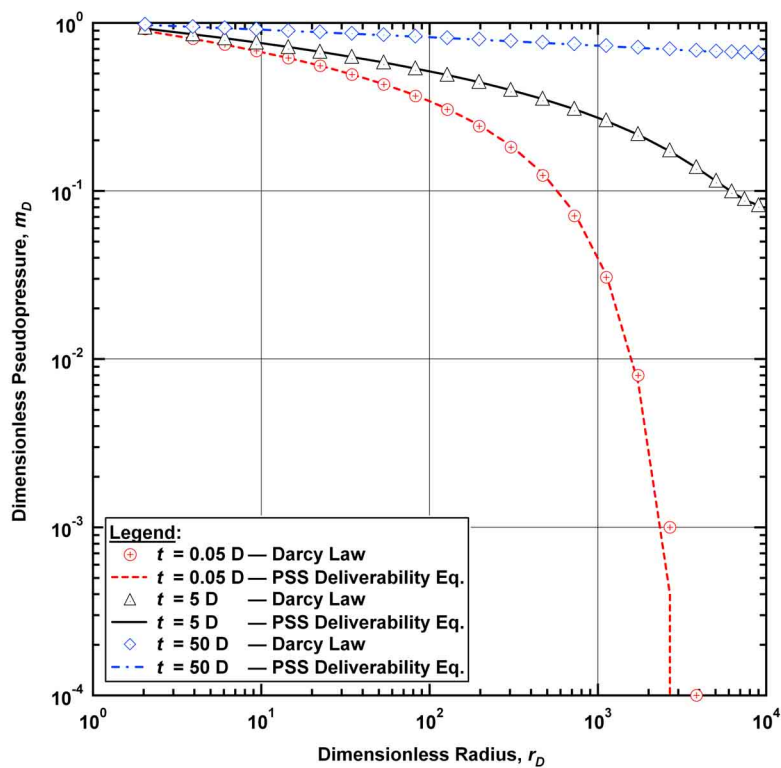


Figure 3.11 — Log-log comparison of pressure profiles predicted by coupling our solution with Darcy's law and the PSS deliverability equation.

This evaluation confirms (again) empirically that the correctness of the computed (pseudo) pressure profiles is a necessary condition of correctness for the rate history.

A logical recommendation for accelerating the procedure consists in using Darcy's law for the transient period (its duration may be exaggerated by supposing it equal to 4-5 times time required for the investigation radius to reach the outer boundary) and the switching to a PSS-type deliverability equation during the boundary-dominated flow regime. Normally, such an approach will yield shorter computation times, as well as correct rate history and correct pressure profiles for any moment of time since earlier we showed that correctness of pressure profiles is a necessary condition of correctness of rate history.

We note that other deliverability equations may also be considered, but any acceleration device (*i.e.*, something that permits larger timesteps (especially, in case of an extreme drawdown) or eliminates the Laplace domain computations) must be thoroughly validated.

CHAPTER IV

EXTENSIONS

The work of Mireles and Blasingame¹ for a constant rate inner boundary condition and the present work for a constant pressure inner boundary condition demonstrate that the Average Pressure Approximation (or APA) is both original and powerful. The question is how powerful — what are the limitations? In particular, can this concept be used to develop a variable rate/variable pressure solution.

Following the logic of Appendix B (*i.e.*, the development of the $g(t)$ function), we can test our concept for cases where linear (or liquid) solutions are well-established — for example, different non-circular geometries, arbitrary position of the well, horizontal well, naturally fractured reservoir. Another consideration would be to add the non-Darcy term and the skin factor into the problem — we note that such additions appear to be straightforward.

We would like to assess the feasibility of using our solution as a gas reservoir "simulator" — *specifically, can we model changing flowrates and/or changing wellbore flowing pressures?* In this chapter we want to demonstrate a possible approach which would allow us to generalize application of our methodology to the case of a well with a changing well bottomhole pressure.

4.1 Initial Attempts to Model a Variable Pressure Schedule

Two initial attempts were made to solve the variable pressure problem in a simplistic fashion, these are:

1. At the moment of the change in wellbore pressure, we propose that the "initial pressure" for the new period (or event) to be equal to the average reservoir pressure at the end of the previous period (or event). In this case, the problem is reduced to a suite of solutions developed and validated earlier in this work (Darcy's law is used for all periods). In this scenario, the inner boundary condition is not time dependent for any problem of this type. This approach yields poor results — particularly if bottomhole pressure successively decreases this approach underestimates the flowrate profiles. Of course this is a consequence of non-uniform initial condition — which is our base assumption for this approach.
2. In our second attempt we use a pseudosteady-state (PSS) deliverability equation for successive events (but not the first event). The results are poor at least in the beginning of a particular event (*i.e.*, during transient flow — as would be expected using the PSS equation). Another characteristic of this solution approach is that if the bottomhole pressure successively decreases, then this approach will always overestimate the rate.

The reservoir system we used is of Type 2 — $r_{eD} = 10^4$ and the pressure schedule is presented in **Table 4.1**. **Figure 4.1** illustrates the performance of the two "simplistic" solution attempts.

Table 4.1 — Flowing Bottomhole Pressure Schedules (Used in Initial Attempts to Model a Variable Pressure Schedule).

Time (D)	Flowing Bottomhole Pressure (psia)
5	4500
10	4400

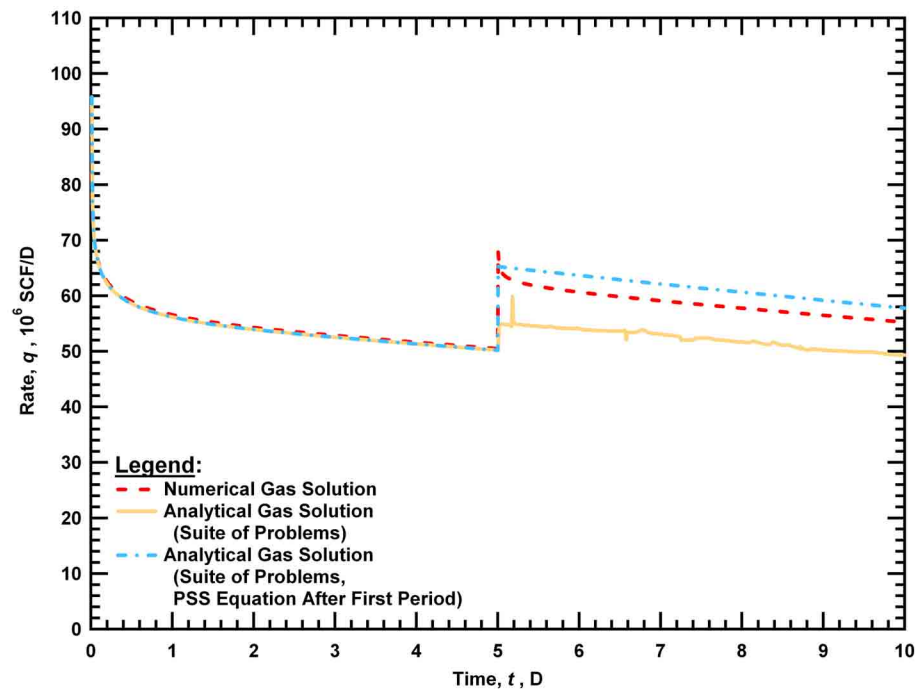


Figure 4.1 — Comparison of "simplistic" strategies used to generate production profiles for the variable bottomhole flowing pressure case.

4.2 Time-Dependent Inner Boundary Condition (Variable Pressure Schedule)

A more theoretical approach is to specifically consider a time dependent inner boundary condition — however, this approach requires a complete recasting of the solution approach. This concept seems to be the most logical and we present the developments in the following section.

As a start, the linear (or liquid) Laplace domain solution is cast in the form of a *time-dependent* inner boundary condition. Fortunately, the nature of the $\bar{g}(u)$ term is invariant with respect to bottomhole

pressure schedule — actually $\bar{g}(u)$ is taken specifically to be a function of the average reservoir pressure — which (obviously) is a function of both time and the bottomhole pressure schedule.

We begin with the dimensionless diffusivity equation in terms of pseudopressure and time:

$$\frac{1}{r_D} \frac{\partial}{\partial r_D} \left[r_D \frac{\partial m_D}{\partial r_D} \right] = \frac{\mu c}{\mu_i c_i} \frac{\partial m_D}{\partial t_D} \dots\dots\dots (4.1)$$

Where dimensionless pseudopressure is defined by:

$$m_D = \frac{m_i - m}{m_i - m_{wf}} \dots\dots\dots (4.2)$$

In our previous developments the dimensionless pseudopressure (m_D) was constrained between 1 ($m = m_{wf}$) and 0 ($m = m_i$). And the inner boundary condition was specifically defined as:

$$m_D \Big|_{r_D=1} = 1 \dots\dots\dots (4.3)$$

Where the condition given by Eq. 4.3 is independent of time. Generalizing, we can write the inner boundary condition for the case of a varying bottomhole pressure schedule as follows:

$$m_D \Big|_{r_D=1} = \sigma(t_D) \dots\dots\dots (4.4)$$

Where $\sigma(t_D)$ is, in general, a superposition of Heaviside functions (*i.e.*, step-changes in the flowing bottom-hole pressure). Applying the Laplace transformation and using the initial condition, we have:

$$\frac{d^2 \bar{m}_D(u)}{dr_D^2} + \frac{1}{r_D} \frac{d\bar{m}_D(u)}{dr_D} = [u\bar{m}_D(u) - m_D(t_D = 0)]\bar{g}(u) \dots\dots\dots (4.5)$$

In this process, the inner boundary becomes:

$$\bar{m}_D = \bar{\sigma}(u) \dots\dots\dots (4.6)$$

And the outer boundary condition becomes:

$$\left[r_D \frac{d\bar{m}_D}{dr_D} \right]_{r_D=r_{eD}} = 0 \dots\dots\dots (4.7)$$

As in our previous development, the solution form of Eq. 4.5 is given as:

$$\bar{m}_D(u) = \bar{g}(u) \int_0^\infty p_D(t_D) e^{-u\bar{g}(u)t_D} dt_D \dots\dots\dots (4.8)$$

or

$$\bar{m}_{D,gas}(u) = \bar{g}(u) \bar{m}_D(u\bar{g}(u)) \dots\dots\dots (4.9)$$

The linear (or liquid) form of the general solution for this problem is defined by:

$$\bar{m}_D(r_D, u) = AI_0(r_D \sqrt{u}) + BK_0(r_D \sqrt{u}) \dots\dots\dots (4.10)$$

Using our boundary conditions, we have:

$$A = \bar{\sigma}(u) \frac{K_1(r_{eD} \sqrt{u})}{K_0(\sqrt{u})I_1(r_{eD} \sqrt{u}) + K_1(r_{eD} \sqrt{u})I_0(\sqrt{u})} \dots\dots\dots (4.11)$$

$$B = \bar{\sigma}(u) \frac{I_1(r_{eD} \sqrt{u})}{K_0(\sqrt{u})I_1(r_{eD} \sqrt{u}) + K_1(r_{eD} \sqrt{u})I_0(\sqrt{u})} \dots\dots\dots (4.12)$$

Substituting Eqs. 4.11 and 4.12 into Eq. 4.10 yields:

$$\bar{m}_D = \frac{1}{u} \frac{K_1(r_{eD} \sqrt{u})I_0(r_D \sqrt{u}) + K_0(r_D \sqrt{u})I_1(r_{eD} \sqrt{u})}{K_0(\sqrt{u})I_1(r_{eD} \sqrt{u}) + K_1(r_{eD} \sqrt{u})I_0(\sqrt{u})} \dots\dots\dots (4.13)$$

We now substitute Eq. 4.13 into Eq. 4.9 to obtain our final form of the solution in the Laplace domain:

$$\bar{m}_{D,gas} = \bar{g}(u) \bar{\sigma}(u \bar{g}(u)) \frac{K_1(r_{eD} \sqrt{u \bar{g}(u)})I_0(r_D \sqrt{u \bar{g}(u)}) + K_0(r_D \sqrt{u \bar{g}(u)})I_1(r_{eD} \sqrt{u \bar{g}(u)})}{K_0(\sqrt{u \bar{g}(u)})I_1(r_{eD} \sqrt{u \bar{g}(u)}) + K_1(r_{eD} \sqrt{u \bar{g}(u)})I_0(\sqrt{u \bar{g}(u)})} \dots\dots\dots (4.14)$$

We note that during the first period of a variable pressure schedule, Eq. 4.14 is equivalent to Eq. A-31 (which is the solution for the constant wellbore pressure case) — in other words, Eq. 4.14 generalizes Eq. A-31 for the variable pressure schedule. To visualize this property, simply recall the Laplace transform of a Heaviside function — *i.e.*, $\bar{\sigma}(u) = 1/u$ for the case of production at a single constant pressure.

Performance testing of Eq. 4.14 yields transient responses in the beginning of every period — but the rates were incorrect — except (of course) for the first period. We believe that this phenomena is related to numerical problems — the APA typically works for much worse conditions (see Appendix B). In this case the bottomhole pressure schedule makes use of Heaviside functions, consequently the Laplace domain solution includes Laplace transforms of Heaviside functions — which discontinuous steps. Numerical inversion of this formulation is challenging to say the least — for example, Fourier-based inversion methods generally provide a good representation of "discrete steps" but often require so many terms that computational precision of the Fourier series is compromised (numerically). Of course it is very easy analytically evaluate the Laplace transform of a Heaviside function, but when the Heaviside function is multiplied by another function in the Laplace domain, the inverse Laplace transformation often becomes problematic in a computational sense (this is a common issue).

With these presumed numerical problems in mind, we attempted (as before) to validate the reservoir pressure profiles computed for a given rate history (which is generated by a numerical simulator) for a specified schedule of flowing bottomhole pressures. We note that these results (**Fig. 4.2**) are *excellent* compared those obtained for the single constant bottomhole flowing pressure case. We believe that any differences which arise in this comparison are due to the use of the Laplace transformation and inverse transformation of the Heaviside functions used to represent the variable pressure case. But we note

(again) that the results shown in **Fig. 4.2** are excellent. For this comparison we use a reservoir of Type 2 ($r_{eD} = 10^4$ and the pressure schedule is given in **Table 4.2**).

Table 4.2 — Flowing Bottomhole Pressure Schedules (Used in Application of a Rigorous Solution Formulation for a Variable Pressure Schedule).

Time (D)	Flowing Bottomhole Pressure (psia)
2.5	4500
5	4400

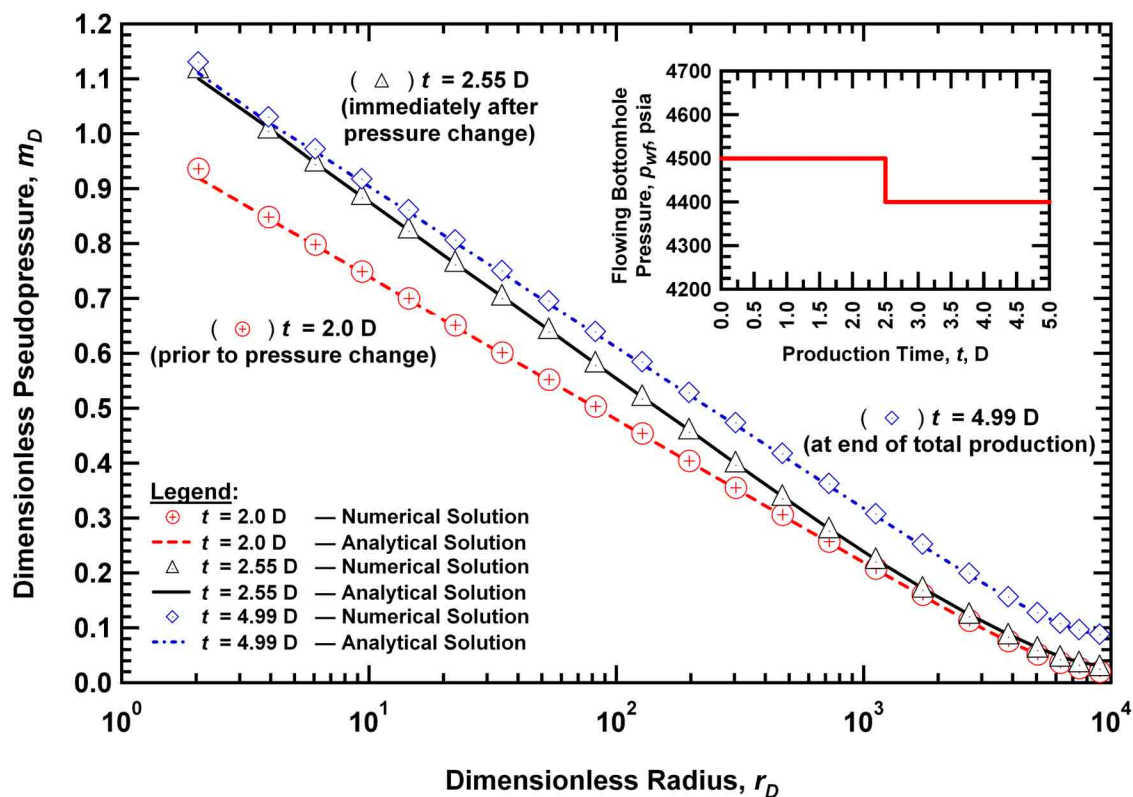


Figure 4.2 — Pressure profile comparison computed based on flowrate profiles obtained from numerical simulation for the variable flowing bottomhole pressure case.

CHAPTER V

SUMMARY, CONCLUSIONS, AND RECOMMENDATIONS FOR FUTURE WORK

5.1 Summary

We have developed a new semi-analytical solution approach for the gas diffusivity equation for the case of a gas well producing at a *constant flowing well bottomhole pressure* in a homogeneous, bounded circular reservoir. We were inspired by Mireles and Blasingame¹ approach for the case of a *constant (sandface) flowrate* condition. Our new approach follows by also *considering the viscosity-compressibility product to be only time-dependent* — where we have assumed (then validated) that the μc product evaluated at average reservoir pressure uniquely represents the time-dependent character of this problem.

Technically, incorporating the average pressure approximation (APA) requires recasting of the right-hand-side of the dimensionless diffusivity equation into a convolution of two independent functions, as well as the subsequent use of the Laplace transformation. The proposed solution is evaluated using the liquid flow solution, coupled with the "real gas" function $\bar{g}(u)$ in the Laplace domain (or $g(t)$ in the real domain, where this is defined by Eq. 2.24) — where specifically, $\bar{g}(u)$ represents the non-linear behavior (*i.e.*, pressure dependency of the thermodynamic properties of the gas). We note that our expression for $\bar{g}(u)$ contains the corresponding expression developed by Mireles and Blasingame¹ for a constant rate inner boundary condition as a particular case within the general definition of $\bar{g}(u)$. The resulting real gas solution (in the Laplace domain) has a form similar to the case of a well in a naturally fractured reservoir — where this makes the interchange between the liquid and real gas flow solutions only dependent on our ability to appropriately calculate $\bar{g}(u)$.

The new solution approach was implemented and verified by comparison with numerical results from a finite-difference simulator. We considered a variety of reservoir and fluid properties, as well as various production schedules. We note excellent comparisons of pressure profiles and rates for all cases which does empirically validate applicability of our approach to gas flow systems.

The approach works well for all scenarios tested (and we note that several scenarios were quite extreme — *i.e.*, $0.02 < p_w/p_i < 0.98$). This leads us to conclude that the APA assumption is not restrictive, but in fact, is the appropriate basis for such solutions. In order to support this empirical verification by theory, we propose an insight into rigorous determination of limits of validity of the APA for both the constant pressure and constant rate inner boundary condition problems. We consider the validity of the APA as an

intrinsic mathematical property of this problem, and we believe that the goal of clarifying this issue is crucial.

More importantly, we considered different extensions (or generalizations) of our solution approach that should allow its application to more complex gas engineering problems. In particular, using our approach, which combines the APA and convolution, we propose a procedure to resolve the time-dependent inner boundary condition gas flow problem (*i.e.*, variable flowing bottomhole pressure problem). The reservoir pressure profiles were correctly calculated using this approach (which we consider to be a necessary condition of the correctness of rate history) — however, when generating flowrate-time profiles we experienced numerical problems apparently caused by inverse the Laplace transformation of discontinuous functions. This remains under study, and is given specifically as a recommendation for future work.

In summary, the primary theoretical difference between this work for a constant wellbore flowing pressure and the original work of Mireles and Blasingame¹ for the constant flowrate problem is the specific formulation of the Laplace domain functional for gas (*i.e.*, the $\bar{g}(u)$ term). In addition, since this work requires "projection" of flowrate at a particular timestep, we used a rate projection based on Darcy's law.

5.2. Conclusions

The most important conclusion of this work is that the APA concept is valid for the constant pressure inner boundary condition gas flow problem. We also believe this concept to be valid for the general case of variable-rate/variable pressure, but this work is ongoing.

In this work we provide the next step beyond the constant rate formulation proposed by Mireles and Blasingame¹ where our new approach for the constant wellbore pressure case also incorporates the APA and convolution. The results of this work provide a solution approach which can be readily incorporated into well test and production data analysis — without using reservoir simulation for the gas flow case. As noted above, we define the next phase of this work — specifically the application of time-dependent inner boundary conditions (in particular, the variable flowing bottomhole pressure problem).

At present, our approach may be used for simple flow problems, as well as for verifying numerical simulator results, or more precisely for assessing adequacy of spatial and temporal discretizations used in the numerical simulator.

5.3 Recommendations for Future Work

We believe that investigation of the following topics will assist in the development the proposed approach into a reliable and robust tool for use in well test and production data analysis, and for modelling the performance of gas reservoirs:

- Average Pressure Approximation (APA): The validity of the APA approach should be rigorously assessed using the functional model presented in Appendix B. An analytical proof of the APA concept (as opposed to our empirical efforts) will provide a common theoretical basis for constant pressure and constant rate production regimes.
- Further Proof-of-Concept: We have established (empirically) that the correctness of the computed pressure profiles (*i.e.*, $p(r)$) is a necessary condition to prove the correctness of rate history. This issue is of methodological importance, but it should be studied further.
- Extension to a Generic Production Schedule: Ultimately, the "product" of this work is an accurate, high-speed computational solution (or "simulator"). As such, we need to develop a robust and functional solution for the case of a general production schedule (*i.e.*, arbitrary rates and pressures). Our efforts to date are documented in Chapter 4 — but we note that at present, we do experience computational difficulties, presumably linked to the inverse Laplace transformation of the "step change" solution. We propose remedies and continue work on this particular problem, but we also encourage other researchers to follow our work — and/or any other extensions which arise from our efforts.
- Other Applications: The proposed solution methodology should be extended to other applications such as more complex geometries, non-Darcy flow, and eventually, to the case of multiphase flow.
- Improvements: We recognize that our work is somewhat fundamental, and that some (or even many) of our computation schemes can be vastly improved with existing and evolving technologies. We encourage others to explore such improvements.

NOMENCLATURE

B	= gas formation volume factor, RCF/SCF
c	= gas compressibility, psia ⁻¹
c_i	= gas compressibility at initial reservoir pressure, psia ⁻¹
\bar{c}	= gas compressibility at average reservoir pressure, psia ⁻¹
D_i	= exponential decline parameter, D ⁻¹
E_1	= exponential integral
G	= gas-in-place, SCF
G_p	= cumulative gas production, SCF
g	= function representing non-linearity of the problem
h	= reservoir height, ft
I_i	= modified Bessel function of first kind of order i
K_i	= modified Bessel function of second kind of order i
k	= effective permeability to gas, md
m	= pseudopressure, psi
m_i	= initial pseudopressure, psi
m_{wf}	= well flowing pseudopressure, psi
p	= pressure, psia
p_{base}	= base pressure in pseudopressure formulation, psia
p_D	= liquid solution term in perturbation technique, psia
p_{wf}	= well flowing pressure, psia
p_0	= initial pressure in Al-Hussainy, Ramey and Crawford ¹⁰ pseudopressure formulation, psia
\bar{p}	= average reservoir pressure, psia
q	= gas flowrate, SCF/D
r_{inv}	= radius of investigation, ft
r	= radial distance, ft
r_e	= external radius, ft
r_w	= wellbore radius, ft
T	= temperature, °F
t	= time, D
t_a	= pseudotime, D
t_0	= initial time in pseudotime formulation, D
z	= z-factor

Dimensionless Variables

m_D = dimensionless pseudopressure

r_D = dimensionless radius

r_{eD} = dimensionless external radius

r_{wD} = dimensionless wellbore radius

t_D = dimensionless time

Greek Letter Variables

β = non-linear viscosity-compressibility function, dimensionless

β_p = non-linear viscosity-compressibility function at average reservoir pressure, dimensionless

γ = gas gravity (air=1)

δ = correction term in perturbation technique

μ = gas viscosity, cp

μ_i = gas viscosity at initial reservoir pressure, cp

$\bar{\mu}$ = gas viscosity at average reservoir pressure, cp

σ = inner boundary condition schedule function

τ = dummy time-type variable, D

ϕ = effective "gas" porosity, fraction

Special Signs and Operators

div = divergence

\mathcal{L} = Laplace transform operator

$\bar{\bullet}$ = Laplace transform

∇ = gradient

Δ = argument increment

REFERENCES

1. Mireles, T.J., and Blasingame, T.A.: "Application of Convolution Theory for Solving Non-Linear Flow Problems: Gas Flow Systems," paper SPE 84073 presented at the 2003 SPE Annual Technical Conference and Exhibition, Denver, CO, 5-8 October.
2. Carslaw, H.S., and Jaeger, J.C.: *Conduction of Heat in Solids*, Oxford at the Clarendon Press, London (1947).
3. Carslaw, H.S., and Jaeger, J.C.: "Some Two-Dimensional Problems in Conduction of Heat with Circular Symmetry," *Proc. London Math. Soc.* (1940) **46**, 361.
4. Jaeger, J.C.: "Heat Flow in the Region Bounded Internally by a Circular Cylinder," *Proc. Royal Soc.* (1942) **61**, 223.
5. Barenblatt, G.I.: *Scaling, Self-similarity, and Intermediate Asymptotics*, Cambridge Texts in Applied Mathematics, Cambridge University Press, Cambridge (1996) **14**.
6. Raghavan, R.: *Well Test Analysis*, Prentice Hall, Englewood Cliffs, NJ (1993).
7. Van Everdingen, A.F. and Hurst, W.: "The Application of the Laplace Transformation to Flow Problems in Reservoirs," *Trans., AIME* (December 1949) **305**.
8. Matthews, C.S., and Russell, D.G.: *Pressure Buildup and Flow Tests in Wells*, Monograph Series, SPE, Richardson, TX (1967) **1**, 25.
9. Aziz, K., Mattar, L., Ko, S., and Brar, G.S.: "Use of Pressure, Pressure-Squared or Pseudo-Pressure in the Analysis of Transient Pressure Drawdown Data from Gas Wells," *JCPT* (April-June 1976) 58.
10. Al-Hussainy, R., Ramey, H.J., Jr., and Crawford, P.B.: "The Flow of Real Gases Through Porous Media," *JPT* (May 1966) 624.
11. Agarwal, R.G.: "Real Gas Pseudo-Time — A New Function for Pressure Buildup Analysis of MHF Wells," paper SPE 8279 presented at the 1979 SPE Annual Technical Conference and Exhibition, New Orleans, LA, 23-26 September.
12. Lee, W.J., and Holditch, S.A.: "Application of Pseudotime to Buildup Test Analysis of Low-Permeability Gas Wells With Long-Duration Wellbore Storage Distortion," *JPT* (December 1982) 2877.
13. Kale, D., and Mattar, L.: "Solution of a Non-Linear Gas Flow Equation by the Perturbation Technique," *JCPT* (October-December 1980) 63.
14. Kabir, C.S., and Hasan, A.R.: "Prefracture Testing in Tight Gas Reservoirs," *SPEFE* (April 1986) 128.
15. Aadnoy, B.S., and Finjord, J.: "Discussion of Prefracture Testing in Tight Gas Reservoirs," *SPEFE* (April 1986) 628.

16. Kikani, J., and Pedrosa, O.A., Jr.: "Perturbation Analysis of Stress-Sensitive Reservoirs," *SPEFE* (September 1991) 379.
17. Wang, Y.: "Discussion of Perturbation Analysis of Stress-Sensitive Reservoirs," *SPEFE* (September 1992) 268.
18. Arps, J.J.: "Analysis of Decline Curves," *Trans.*, AIME (December 1945) **228**.
19. Fetkovich, M.J.: "Decline Curves Analysis Using Type Curves," paper SPE 4629 presented at the 1973 SPE Fall Meeting, Las Vegas, NV, 30 September-3 October.
20. Ansah, J., Knowles, R.S., and Blasingame, T.A.: "A Semi-Analytic (p/z) Rate-Time Relation for the Analysis and Prediction of Gas Well Performance," *SPERC* (December 2000), 525.
21. Buba, I.M., and Blasingame, T.A.: "Direct Estimation of Gas Reserves Using Production Data," paper SPE 77550 presented at the 2002 Annual SPE Technical Conference and Exhibition, San Antonio, TX, 30 September-3 October.
22. Rawlins, E.G., and Schellhardt, M.A.: *Back-Pressure Data on Natural Gas Wells and Their Application to Production Practices*, Monograph Series, U.S. Bureau of Mines (1935) 7, 8.
23. Aronofsky, J.S., and Jenkins, R.: "A Simplified Analysis of Unsteady Radial Gas Flow," *JPT* (May 1954) 321; *Trans.*, AIME, **201**.
24. Rouboutsos, A., and Stewart, G.: "A Direct Deconvolution or Convolution Algorithm for Well Test Analysis," paper SPE 18157 presented at the 1988 SPE Annual Technical Conference and Exhibition, Houston, TX, 2-5 October.
25. Stehfest, H.: "Numerical Inversion of Laplace Transforms," *Communications of the ACM* (January 1970) 47. (Algorithm 368 with correction (October 1970).)
26. Warren, J.E., and Root, P.J.: "The Behavior of Naturally Fractured Reservoirs," *SPEJ* (September 1963) 245; *Trans.*, AIME, **228**.
27. Thompson, L.G., Manrique, J.L., and Jelmert, T.A.: "Efficient Algorithms for Computing the Bounded Reservoir Horizontal Well Pressure Response," paper SPE 21827 presented at the 1991 Joint Rocky Mountain Regional/Low Permeability Reservoirs Symposium, Denver, CO, 15-17 April.
28. Blasingame, T.A., Johnston, J.L., Lee, W.J., and Raghavan, R.: "The Analysis of Gas Well Test Data Distorted by Wellbore Storage Using an Explicit Deconvolution Method," paper SPE 19099 presented at the 1989 Gas Technology Symposium, Dallas, TX, 7-9 June.
29. De Hoog, F.R., Knight, J.H., and Stokes, A.N.: "An Improved Method for Numerical Inversion of Laplace Transforms," *SIAM J. Sci. Stat. Comput.* (September 1982) 357.
30. *Matlab* (software) Version 6.5, MathWorks, Natick, MA (2002).
31. Wattenbarger, R.A.: User's Manual: *Gassim: 2-Dimensional, Real Gas Simulator*, Texas A&M University, College Station, TX (2002).

32. Carter, R.D.: "Type Curves for Finite Radial and Linear Gas Flow Systems: Constant Terminal Pressure Case," *SPEJ* (October 1985) 719.
33. Dranchuk, P.M., and Abou-Kassem, J.H.: "Calculation of z -Factors for Natural Gases Using Equations of State," *JCPT* (July-September 1975) 34.
34. Lee, A.L., Gonzalez, M.H., and Eakin, B.E.: "The Viscosity of Natural Gases," *JPT* (August 1966) 997; *Trans.*, AIME, **237**.
35. Piper, L.D., McCain, W.D., and Corredor, J.H.: "Compressibility Factors for Naturally Occurring Petroleum Gases," paper SPE 26668 presented at the 1993 SPE Annual Technical Conference and Exhibition, Houston, TX, 3-6 October.
36. Sutton, R.P.: "Compressibility Factors for High-Molecular-Weight Reservoir Gases," paper SPE 14265 presented at the 1985 SPE Annual Technical Conference and Exhibition, Las Vegas, NV, 22-25 September.

APPENDIX A

ANALYTICAL PRESSURE SOLUTION

FOR THE CASE OF A CONSTANT PRESSURE

INNER BOUNDARY CONDITION

For clarity we will formulate the problem under study in terms of effective "gas" porosity and will neglect residual water compressibility. Also, rock compressibility (*i.e.*, dependence of porosity on pressure) will be neglected. It is evident that our method could be generalized to account for the compressibility effects stated above. Our assumptions are reasonable because residual water and rock compressibility related effects are typically of second order compared to gas expansion (for gas reservoirs) — with the noted exception being abnormally pressured gas reservoirs. Finally, permeability is supposed constant and independent of pressure.

Combining the continuity equation, Darcy's law and the definition of isothermal compressibility (for a gas), and making use of the following definition of pseudopressure:

$$m = \frac{\mu_i z_i}{p_i} \int_{p_{base}}^p \frac{p}{\mu z} dp \dots\dots\dots (A-1)$$

we construct the diffusivity equation in terms of pseudopressure:

$$\frac{\partial^2 m}{\partial r^2} = \frac{\phi c \mu}{k} \frac{\partial m}{\partial t} \dots\dots\dots (A-2)$$

In order to make the equation above dimensionless we apply the following definitions of dimensionless variables:

$$t_D = t_{DC} \frac{k}{\phi \mu_i c_i r_w^2} t \dots\dots\dots (A-3)$$

where t_{DC} equals 0.0002637 or 0.00633 if time is expressed in hours or days, respectively,

$$r_D = \frac{r}{r_w} \dots\dots\dots (A-4)$$

$$m_D = \frac{m_i - m}{m_i - m_{wf}} \dots\dots\dots (A-5)$$

We note that $m_D = 1$ when $m = m_{wf}$ and 0 when $m = m_i$.

The diffusivity equation in dimensionless form is:

$$\frac{1}{r_D} \frac{\partial}{\partial r_D} \left[r_D \frac{\partial m_D}{\partial r_D} \right] = \frac{\mu c}{\mu_i c_i} \frac{\partial m_D}{\partial t_D} \dots\dots\dots (A-6)$$

Note that using the typical dimensionless group for pseudopressure for constant rate condition:

$$m_D = 25.148 \frac{q B_i \mu_i}{k h} (m_i - m) \dots\dots\dots (A-7)$$

yields a dimensionless equation identical to Eq. A-6. Obviously, this is due to linearity of both definitions of dimensionless pseudopressure.

Eq. A-6 is conditioned as follows. Initial condition:

$$m_D(t_D = 0) = 0 \dots\dots\dots (A-8)$$

Inner boundary condition (constant flowing well bottomhole pressure production):

$$[m_D]_{r_D=1} = 1 \dots\dots\dots (A-9)$$

Outer boundary condition (no-flow boundary):

$$\left[r_D \frac{dm_D}{dr_D} \right]_{r_D=r_{eD}} = 0 \dots\dots\dots (A-10)$$

since by construction the pseudopressure is essentially a potential function and its gradient is proportional to its flux (see also Appendix D).

We define:

$$\beta = \frac{\mu c}{\mu_i c_i} \dots\dots\dots (A-11)$$

(β depends on pressure, and thus, in a context of production from a reservoir, on position and time). Now, the right-hand side of Eq. A-6 can be rewritten as:

$$\beta(t_D) \frac{\partial m_D}{\partial t_D}(t_D) = \int_0^{t_D} \frac{\partial m_D}{\partial \tau}(\tau) g(t_D - \tau) d\tau \dots\dots\dots (A-12)$$

Applying the Laplace transformation to Eq. A-6 we obtain:

$$\frac{d^2 \bar{m}_D(u)}{dr_D^2} + \frac{1}{r_D} \frac{d\bar{m}_D(u)}{dr_D} = [u \bar{m}_D(u) - m_D(t_D = 0)] \bar{g}(u) \dots\dots\dots (A-13)$$

Inner boundary condition becomes:

$$\bar{m}_D = \frac{1}{u} \dots\dots\dots (A-14)$$

and outer boundary condition becomes:

$$\left[r_D \frac{d\bar{m}_D}{dr_D} \right]_{r_D=r_{eD}} = 0 \dots\dots\dots (A-15)$$

One of the most important points is that it can be shown by induction²⁶⁻²⁷ that:

$$\bar{m}_D(u) = \bar{g}(u) \int_0^\infty p_D(t_D) e^{-u\bar{g}(u)t_D} dt_D \dots\dots\dots (A-16)$$

or

$$\bar{m}_{D, gas}(u) = \bar{g}(u) \bar{m}_D(u\bar{g}(u)) \dots\dots\dots (A-17)$$

where \bar{m}_D is the dimensionless Laplace domain linear ("liquid" or "slightly compressible") solution. In fact, Eq. A-13 looks exactly like the equation that can be derived for fractured (double porosity) reservoirs.

The linear solution can be easily constructed in analytical form for our boundary conditions. Multiplying both sides of Eq. A-13 by r_D^2 we obtain:

$$r_D^2 \frac{d^2 \bar{m}_D(u)}{dr_D^2} + r_D \frac{d\bar{m}_D(u)}{dr_D} = r_D^2 u \bar{g}(u) \bar{m}_D \dots\dots\dots (A-18)$$

Making the following transformation of variable:

$$z = r_D \sqrt{u} \dots\dots\dots (A-19)$$

such that:

$$\frac{d \bullet}{dr_D} = \sqrt{u} \frac{d \bullet}{dz} \dots\dots\dots (A-20)$$

we have:

$$z^2 \frac{d^2 \bar{m}_D}{dz^2} + z \frac{d\bar{m}_D}{dz} = z^2 \bar{g} \bar{m}_D \dots\dots\dots (A-21)$$

Eq. A-21 is a modified Bessel equation allowing the following general solution:

$$\bar{m}_D(r_D, u) = AI_0(r_D \sqrt{u}) + BK_0(r_D \sqrt{u}) \dots\dots\dots (A-22)$$

Since

$$\left[r_D \frac{d\bar{m}_D}{dr_D} \right] = Ar_D \sqrt{u} I_1(r_D \sqrt{u}) - Br_D \sqrt{u} K_1(r_D \sqrt{u}) \dots\dots\dots (A-23)$$

and making use of boundary conditions:

$$\frac{1}{u} = AI_0(\sqrt{u}) + BK_0(\sqrt{u}) \dots\dots\dots (A-24)$$

$$0 = Ar_{eD} \sqrt{u} I_1(r_{eD} \sqrt{u}) - Br_{eD} \sqrt{u} K_1(r_{eD} \sqrt{u}) \dots\dots\dots (A-25)$$

we obtain after few simple manipulations:

$$A = \frac{1}{u} \frac{K_1(r_{eD}\sqrt{u})}{K_0(\sqrt{u})I_1(r_{eD}\sqrt{u}) + K_1(r_{eD}\sqrt{u})I_0(\sqrt{u})} \dots\dots\dots (A-26)$$

$$B = \frac{1}{u} \frac{I_1(r_{eD}\sqrt{u})}{K_0(\sqrt{u})I_1(r_{eD}\sqrt{u}) + K_1(r_{eD}\sqrt{u})I_0(\sqrt{u})} \dots\dots\dots (A-27)$$

Finally, we have:

$$\bar{m}_D = \frac{1}{u} \frac{K_1(r_{eD}\sqrt{u})I_0(r_D\sqrt{u}) + K_0(r_D\sqrt{u})I_1(r_{eD}\sqrt{u})}{K_0(\sqrt{u})I_1(r_{eD}\sqrt{u}) + K_1(r_{eD}\sqrt{u})I_0(\sqrt{u})} \dots\dots\dots (A-28)$$

and

$$\bar{m}_{D,gas} = \frac{1}{u} \frac{K_1(r_{eD}\sqrt{u\bar{g}(u)})I_0(r_D\sqrt{u\bar{g}(u)}) + K_0(r_D\sqrt{u\bar{g}(u)})I_1(r_{eD}\sqrt{u\bar{g}(u)})}{K_0(\sqrt{u\bar{g}(u)})I_1(r_{eD}\sqrt{u\bar{g}(u)}) + K_1(r_{eD}\sqrt{u\bar{g}(u)})I_0(\sqrt{u\bar{g}(u)})} \dots\dots\dots (A-29)$$

APPENDIX B

NON-LINEARITY AND AVERAGE PRESSURE APPROXIMATION

B-1 Non-Linear Term

Non-linearity of the problem is represented by (or reduced to) $\bar{g}(u)$.

Chain rule (for differentiation of a composite function) yields:

$$\frac{\partial m_D}{\partial t_D} = \frac{\partial m_D}{\partial m} \frac{\partial m}{\partial p} \frac{\partial p}{\partial(p/z)} \frac{\partial(p/z)}{\partial t} \frac{\partial t}{\partial t_D} \dots\dots\dots (B-1)$$

We calculate all multipliers in the right-hand side of Eq. B-1:

$$\frac{\partial m_D}{\partial m} = -\frac{1}{m_i - m_{wf}} \dots\dots\dots (B-2)$$

$$\frac{\partial m}{\partial p} = \frac{\mu_i z_i}{p_i} \frac{p}{\mu z} \dots\dots\dots (B-3)$$

$$\frac{\partial p}{\partial(p/z)} = \frac{1}{c} \frac{z}{p} \dots\dots\dots (B-4)$$

The gas material balance equation is given by:

$$\frac{\bar{p}}{\bar{z}} = \frac{p_i}{z_i} \left[1 - \frac{G_p}{G} \right] \dots\dots\dots (B-5)$$

and, since for the constant pressure production regime $G_p(t) = \int_0^t q(\tau) d\tau$, we obtain:

$$\frac{\partial(\bar{p}/\bar{z})}{\partial t} = -\frac{p_i}{z_i G} \frac{\partial}{\partial t} \left[\int_0^t q(\tau) d\tau \right] = -\frac{p_i}{z_i G} q(t) \dots\dots\dots (B-6)$$

We substitute $\frac{\partial(p/z)}{\partial t}$ with its average pressure analogue.

The last multiplier follows from the definition of the dimensionless time:

$$\frac{\partial t_D}{\partial t} = t_{DC} \frac{k}{\phi \mu_i c_i r_w^2} \dots\dots\dots (B-7)$$

Assembling Eqs. B-2 through B-7 we have:

$$\frac{\partial m_D}{\partial t_D} = -\frac{1}{m_i - m_{wf}} \frac{\mu_i z_i}{p_i} \frac{p}{\mu z} \frac{z}{p} \frac{1}{c} \left[-\frac{p_i}{z_i G} q(t) \right] \left[\frac{1}{t_{DC}} \frac{\phi \mu_i c_i r_w^2}{k} \right] = \frac{1}{t_{DC}} \frac{1}{m_i - m_{wf}} \frac{\mu_i^2 c_i}{\mu c} \frac{\phi r_w^2}{k G} q(t) \dots\dots\dots (B-8)$$

Recall that we can write:

$$\beta(t_D) \frac{\partial m_D}{\partial t_D} = \int_0^{t_D} \frac{\partial m_D}{\partial \tau} g(t_D - \tau) d\tau \dots\dots\dots (B-9)$$

Here still we do not neglect both spatial and temporal dependence of β -function defined as:

$$\beta = \frac{\mu c}{\mu_i c_i} \dots\dots\dots (B-10)$$

Substitution of Eq. B-8 into Eq. B-9 yields:

$$\frac{\mu c}{\mu_i c_i} \frac{1}{t_{DC}} \frac{1}{m_i - m_{wf}} \frac{\mu_i^2 c_i}{\mu c} \frac{\phi r_w^2}{kG} q(t) = \int_0^{t_D} \left[\frac{1}{t_{DC}} \frac{1}{m_i - m_{wf}} \frac{\mu_i^2 c_i}{\mu c} \frac{\phi r_w^2}{kG} q(\tau) \right] g(t_D - \tau) d\tau \dots\dots\dots (B-11)$$

and after reduction of like terms we have:

$$q = \int_0^{t_D} \left[\frac{\mu_i c_i}{\mu c} q \right] g(t_D - \tau) d\tau \dots\dots\dots (B-12)$$

Now, we introduce the APA (*i.e.*, referencing to average reservoir pressure):

$$\beta_{\bar{p}} = \frac{\bar{\mu c}}{\mu_i c_i} \dots\dots\dots (B-13)$$

such that we eliminate dependence on position, and the right-hand side of the diffusivity equation depends only on time. It follows that:

$$q(t_D) = \int_0^{t_D} \left[\frac{q}{\beta_{\bar{p}}}(\tau) \right] g(t_D - \tau) d\tau \dots\dots\dots (B-14)$$

Finally, property of convolution provides the following expression for $\bar{g}(u)$:

$$\mathcal{L}[g(t_D)] \equiv \bar{g}(u) = \frac{\mathcal{L}[q(t_D)]}{\mathcal{L}\left[\frac{q}{\beta_{\bar{p}}}(t_D)\right]} \dots\dots\dots (B-15)$$

B-2 Nature and Limits of Validity of Average Pressure Approximation

Although one could think of the APA as "natural" and "sound," such "faith" is clearly not enough, and a rigorous explanation of why it works is required. For example, during PSS regime the average pressure is in a sense representative. However, two questions immediately arise — (i) why does the approach work during transient period? (ii) by construction, for constant pressure case the near-wellbore zone is never in PSS (as defined by $dp/dt = \text{constant}$), but since we obtain correct rates which depend on pressure gradient (within the framework of Darcy's law), we do get correct solution even in the zone where p_{avg} is not very representative, why?

In fact, the validity of our APA-based approach is due to a mathematical property of the diffusivity equation — its *insensitivity* to radial variations in β -function.

We have to assess validity of the APA for different reservoir properties and sizes, and fluid properties. The best way to do so is to understand its nature, formalize this understanding and not to make numerical tests for all possible combinations of properties. Understanding of nature of this approximation will also help us to explain why it worked for constant rate case — that is the developments below are pertinent to both production regimes — and more importantly is required to apply the method to time-dependent inner boundary conditions.

Let's have a closer look on Eqs. B-11 to B-14. It is easy to see that those developments are *equivalent* to calculating β -function inside the expression for $\frac{\partial m_D}{\partial t_D}$ at average pressure, and then making the same

assumption for the independent β -function in Eq. B-9. It is important to note that in such a case the temporal derivative of dimensionless pseudopressure would be estimated quite correctly — despite two approximations (Eq. B-6 and calculation of β -function in Eq. B-8 at average pressure) made to calculate it.

In fact, it appears (at least empirically) that using Eq. B-6 leads to overestimating the temporal derivative of dimensionless pseudopressure in the vicinity of the wellbore and underestimating of it for larger radii, while calculating β -function in Eq. B-8 at average pressure inversely leads to underestimating the temporal derivative of dimensionless pseudopressure in the vicinity of the wellbore and overestimating of it for larger radii. Thus, these two effects counteract and it can be quite confidently conjectured that the validity of our approach depends *in first approximation* only on the validity of the APA applied to the independent β -function in Eq. B-9. Below, we discuss the latter issue.

Suppose that the replacement of

$$\beta = \frac{\mu c}{\mu_i c_i} \dots\dots\dots (B-16)$$

which depends on pressure and thus on time and position (radius in our case of radial geometry), by

$$\beta_{\bar{p}} = \frac{\overline{\mu c}}{\mu_i c_i} \dots\dots\dots (B-17)$$

which obviously depends only on time, is absolutely legitimate. In such an ideal case our developments will be exactly true.

For a particular reservoir-production system we analyzed profiles of β -function for different times and compared them to the value of β -function at the average pressure at the same time. We noticed that the maximum deviation from the value of β -function at the average pressure is localized near the wellbore. The maximum deviation tends to zero while average pressure tends to the flowing well bottomhole pressure (*i.e.*, while pressure profiles become "more uniform").

On the other hand, our method yielded accurate results even for very large drawdowns. It means that the diffusivity equation is not sensitive to the deviations from the average pressure values of β -function (**Fig. B-1**). A rigorous approach to test the degree of insensitivity is to model the real β -function as a superposition of the average-pressure value and a deviation function depending on radius and time in a manner similar to what happens in real cases.

$$\beta(t_D, r_D) = \beta_{\bar{p}}(t_D) + \delta(t_D, r_D) \dots\dots\dots (B-18)$$

The goal is to determine the limits on the deviation function δ and to establish correspondence between limiting δ functions and reservoir properties and production constraints.

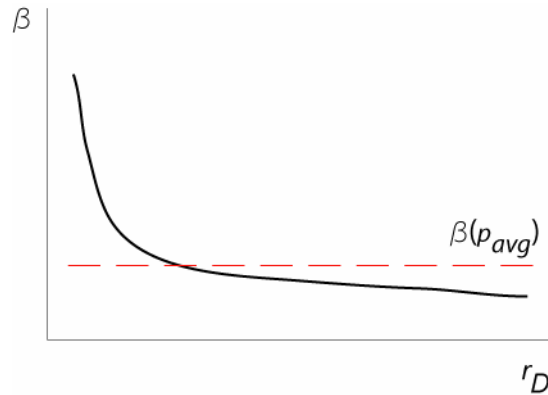


Figure B-1 — Typical profile of β -function during production (for both constant pressure and constant rate inner boundary conditions).

In order to choose an adequate deviation function one has to study behavior of the non-linear viscosity-compressibility function with pressure, temperature, and composition in context of pressure profiles occurring during production. It should be underlined however, that, unfortunately, the ordinary differential equation that we obtain after Laplace transformation of the diffusivity equation with β -function given by Eq. B-18 is not anymore a Bessel differential equation but a more complex one. Its solution may be expressed in terms of Laguerre polynomials and hypergeometric functions, and packages of symbolic mathematics are required for ease of manipulation. *In extremis*, such analysis can become as computational as empirical testing (comparison with numerical simulator solution); consequently, for the sake of practicality we would prefer the latter applied to a carefully chosen set of experiments.

APPENDIX C
ADAPTED ROUMBOUTSOS AND STEWART NUMERICAL
LAPLACE TRANSFORM ALGORITHM

Often we ignore the functional value at $t = 0$ and therefore values between $t = 0$ and the first time point t_1 where the value is known, whereas these values are necessary to calculate the Laplace transform of the function:

$$\bar{f}(s) = \int_0^\infty f(t) \exp(-st) dt \dots\dots\dots (C-1)$$

Improper estimation of functional values between $t = 0$ and t_1 leads after inverse Laplace transformation to an artifact for $t \leq t_1$ as reported by Mireles and Blasingame.¹

Since piece-wise linear approximation of the function to be transformed used in Roumboutsos and Stewart²⁴ algorithm proved sufficiently accurate for the purpose of this work, we will assume such approximation in the following. In any case, the basic idea can be readily generalized to splines or other types of interpolation wherever their application is required.

One way of extrapolating values of the function into $[0, t_1]$ is to impose $f(t = 0) = 0$. However, it is not the best approach, especially for decrescent functions. We propose to simply extrapolate the linear segment constructed between t_1 and t_2 . Therefore, we can make the following developments.

In practice we are given functional values $f_1 \dots f_{n+1}$ for $(n+1)$ argument values. The piece-wise linear approximation is defined by:

$$f(t) = f_i(t) \quad \text{for } t \in [t_i, t_{i+1}] \dots\dots\dots (C-2)$$

$$f_i(t) = f_i + \dot{f}_i(t - t_i) \dots\dots\dots (C-3)$$

$$\dot{f}_i(t) = \frac{f_{i+1} - f_i}{t_{i+1} - t_i} \dots\dots\dots (C-4)$$

where $i = 1 \dots n$.

Laplace transformation of Eq. C-2 yields:

$$\bar{f}(s) = \sum_{i=1}^n \bar{f}_i(s) \dots\dots\dots (C-5)$$

where terms are given by:

$$\bar{f}_i(s) = \int_{t_i}^{t_{i+1}} f_i(t) \exp(-st) dt = \int_{t_i}^{t_{i+1}} [f_i + \dot{f}_i(t - t_i)] \exp(-st) dt =$$

$$= \frac{f_i}{s} \exp(-st_i) - \frac{f_{i+1}}{s} \exp(-st_{i+1}) + \frac{\dot{f}_i}{s^2} [\exp(-st_i) - \exp(-st_{i+1})] \dots \dots \dots (C-6)$$

except the first

$$\dot{f}_1(s) = \frac{1}{s} (f_1 - \dot{f}_1 t_1) + \frac{\dot{f}_1}{s^2} [1 - \exp(-st_2)] - \frac{f_2}{s} \exp(-st_2) \dots \dots \dots (C-7)$$

and the last

$$\bar{f}_n(s) = \frac{f_n}{s} \exp(-st_n) + \frac{\dot{f}_n}{s^2} \exp(-st_n) \dots \dots \dots (C-8)$$

Combining Eqs. C-5 to C-8 we have

$$\dot{f}(s) = \frac{1}{s} (f_1 - \dot{f}_1 t_1) + \frac{\dot{f}_1}{s^2} [1 - \exp(-st_2)] + \frac{1}{s^2} \sum_{i=2}^{n-1} \dot{f}_i [\exp(-st_i) - \exp(-st_{i+1})] + \frac{\dot{f}_n}{s^2} \exp(-st_n) \dots (C-9)$$

Of course, the equation above will also hold when $t_1 = 0$. Note that it extrapolates the last segment linearly to infinity with a slope determined by the last two functional values. If we know that for $t \geq t_{n+1}$ function is constant than by adding an extra point with the same value as $f(t_{n+1})$ will make results of Eq. C-9 accurate for all $t > 0$.

In the context of this work we are interested in functions of the following type:

$$f : [0, t] \rightarrow R_+ \dots \dots \dots (C-10)$$

Indeed, during performance prediction after every time increment we calculate the pressure profile (or more precisely, pressure at a point in the vicinity of the wellbore such that finite difference approximation to the pressure gradient in Darcy's law, if we use the latter as the deliverability equation, is valid) based on the rate history antecedent to this time increment, and actualize the value of rate. Note that we do not know the rate history beyond the current time increment. So one could propose to consider such functions to be defined on a compact support (*i.e.*, to impose $f=0$ for $t > t_{\text{current}}$), for example. Laplace transform of such a function can be calculated either adding two time points with zero functional values and using Eq. C-9, or by using the following equation without adding extra points:

$$\dot{f}(s) = \frac{1}{s} (f_1 - \dot{f}_1 t_1) + \frac{\dot{f}_1}{s^2} [1 - \exp(-st_2)] + \frac{1}{s^2} \sum_{i=2}^n \dot{f}_i [\exp(-st_i) - \exp(-st_{i+1})] - \frac{f_{n+1}}{s} \exp(-st_{n+1}) \dots \dots (C-11)$$

However, the values of the function to be transformed beyond a given value of the argument are irrelevant if after required manipulations its inverse transform is calculated for values not greater than that value of argument, which is the case for us. The only concern is computational — the extrapolation of the function to infinity should not lead to infinite values of the Laplace transform or/and to too small values if it is involved in division. Since we use linear approximation the infinite-support term respects these computational conditions. Moreover, it is advisable to prefer linear extrapolation to infinity as in Eq. C-9

over the compact-support formulation of Eq. C-11 for performance prediction, because numerical inversion of Laplace transforms of functions containing discontinuities in the vicinity of the discontinuities may lead to erroneous values. For example, we observed some "instabilities" of the rate. Yet another argument in favor of using the infinite-support term is that being continuous the function is inverted more efficiently — Fourier-type inversion algorithm, for example, requires less Fourier terms and converges quicker.

APPENDIX D

ALGORITHMS FOR VERIFICATION AND PERFORMANCE PREDICTION: ACCURACY AND COMPUTATIONAL TIME CONSIDERATIONS

In this Appendix we briefly discuss key points of two algorithms developed and implemented for pressure profiles verification and performance prediction, respectively.

Our algorithms and corresponding programs have modular structure that simplifies design and testing but sometimes has negative implications on computational time. The main subprograms or stages of algorithms are:

- Thermodynamic properties.
- Laplace transformation.
- Inverse Laplace transformation.
- Optimization or root finding.
- Integration.

Thermodynamic properties were generated using Dranchuk and Abou-Kassem³³ correlation for z -factor (and consequently for gas compressibility) and Lee, Gonzalez, Eakin³⁴ correlation for gas viscosity. Pseudocritical properties were calculated according to the correlation proposed by Piper, McCain and Corredor.³⁵ Thus, one can test our programs (and our methodology) on different gases within the limits of validity of correlations used:

- CO₂, H₂S and N₂ impurities are allowed.
- Pressure in a very wide range up to 15000 psia.
- Temperatures from 50 to 350°F.
- Gas gravities from 0.55 to 1.

Gas formation volume factor was calculated as:

$$B = \frac{(T + 459.67)z p_{sc}}{(T_{sc} + 459.67)p} \dots\dots\dots (D-1)$$

Laplace transformation was performed using Rouboutsos and Stewart²⁴ algorithm taking into account commentaries given in Appendix C. This algorithm approximates the function to be transformed with a piece-wise linear function.

Inverse Laplace transformation was performed using de Hoog, *et al.*²⁹ algorithm. This Fourier-series-based algorithm was chosen because of its accuracy when dealing with discontinuous functions.

Optimization or root finding were necessary to find the corresponding value of pressure given a value of p/z ratio or pseudopressure.

Based on our algorithms we wrote two programs for *Matlab*. Two main requirements on our programs were high accuracy and low computational time. Modular implementation allowed independent checking of subprograms for accuracy. Thus, we checked the main stages of algorithms — in particular, Laplace and inverse Laplace transformation procedures.

In the beginning of the development cycle our programs were not computationally efficient and algorithms had to be optimized. Conveniently, *Matlab* has a tool known as Profiler which calculates processor time consumed by every function or subprogram. We found that the most time-consuming functions were:

- File input and output.
- Integration.
- Optimization (or root finding). Note that root finding and optimization both were used `find roots` and appeared to be of comparable efficiency.
- Functions calculating gas properties were called too often (recall that Dranchuk and Abou-Kassem correlation is iterative and therefore computationally intense).

Firstly, we eliminated all file operations except final result output and replaced them by dynamically transferring an array containing rate history and β -function values versus time. We also eliminated the majority of "for" loops in our code profiting from what is known in *Matlab* as *vectorization* of operations.

Furthermore, it is easy to see that given the definition of dimensionless pseudopressure for constant pressure production (Eq. 2.9), p_{base} in the definition of pseudopressure (Eq. 2.10) is irrelevant and an arbitrary value can be used — of course, using p_{base} values close to p_i is the most efficient.

At every timestep we need to calculate the corresponding value of pressure given a value of p/z ratio obtained from material balance. If we use an optimization procedure we have to provide range of pressure values to look in. Taking into account the value of average pressure and rate at the end of the previous timestep and the duration of current timestep, the range of pressures for optimization was strongly narrowed.

The changes above yielded very significant gains in computational time. A comparable gain came from a change in calculating the rate. Recall that the latter is given by Darcy's law:

$$q = \frac{1}{25.148} \frac{kh}{B\mu} r \frac{\partial p}{\partial r} \dots\dots\dots (D-2)$$

Since the diffusivity equation given by Eq. 2.11 is formulated in terms of dimensionless pseudopressure, at first after obtaining the value of dimensionless pseudopressure we were calculating the pseudopressure:

$$m = m_i - m_D(m_i - m_{wf}) \dots\dots\dots (D-3)$$

and the corresponding value of pressure. This required optimization or root finding and was showed to be one of the bottlenecks by the Profiler.

It is easy to see using the chain rule that:

$$\frac{\partial m}{\partial r_D} = \frac{\partial m}{\partial p} \frac{\partial p}{\partial r_D} \dots\dots\dots (D-4)$$

where

$$\frac{\partial m}{\partial p} = \frac{\mu_i z_i}{p_i} \frac{p}{\mu z} \dots\dots\dots (D-5)$$

So, we can write:

$$\left. \frac{\partial p}{\partial r_D} \right|_{r_D=1} = \frac{[\partial m / \partial r_D]_{r_D=1}}{[\partial m / \partial p]_{r_D=1}} = \frac{m(1 + \Delta r_D) - m(1)}{\Delta r_D} \dots\dots\dots (D-6)$$

$$\frac{\mu_i z_i}{p_i} \frac{P_{wf}}{(\mu z)_{p=P_{wf}}}$$

Thus, the need for optimization or root finding for calculating rate was eliminated. We note also that an analytical expression can be derived for the gradient of the Laplace transform of the dimensionless pseudopressure — this may lead to additional gains in computational time.

Although our programs after changes described above perform competitively fast and accurately, the following issue have to be addressed:

- Estimation of complexity of the algorithm at timestep n .
- Taking less intermediary knots for Rouboutsos and Stewart algorithm at higher n .
- Optimization of calls to functions which calculate thermodynamic properties.
- Choosing optimal timestep scheduling for given reservoir properties and production constraints.
- Alternative inverse Laplace transform algorithms.

Overall, it is a very compact modular-structure program that works very fast and reliably, and still can be improved for speed of calculation.

VITA

Name: Mansur Zhakupov
Born: 15 May 1981
Astana (Kazakhstan)
Permanent Address: 66 Saryarka Street, Apt. 55
Astana 010000
Kazakhstan
(mansur.zhakupov@m4x.org)
Education: Ecole Polytechnique, Palaiseau, France
Ingénieur de l'Ecole Polytechnique
September 2003
Texas A&M University, College Station, Texas, USA
Master of Science Degree in Petroleum Engineering
May 2005